From Vauquelin's and Magnus' Salts to Gels, Uniaxially Oriented Films, and Fibers: Synthesis, Characterization, and Properties of Tetrakis(1-aminoalkane)metal(II) Tetrachlorometalates(II)

Juliane Bremi, Dorothee Brovelli, Walter Caseri,* Georg Hähner, Paul Smith, and Theo Tervoort

Department of Materials, ETH Zentrum, CH-8092 Zürich, Switzerland

Received September 14, 1998. Revised Manuscript Received December 22, 1998

Complexes of the type $[Pt(NH_2R)_4][PtCl_4]$ with $R = (CH_2)_nCH_3$, where *n* is 3, 6, 7, 8, 9, 11, or 13, were synthesized and characterized with various methods (e.g., IR spectroscopy, SAXS, XPS, NEXAFS, TEM, DSC, and TGA). For comparison, the classical Magnus' green and pink salt (where R = H) were also prepared. The designated alkyl-substituted platinum compounds are pink, but their structure seems to be related rather with Magnus' green than with the pink salt. However, the Pt−Pt distance in the pink alkyl-substituted compounds is most likely larger than in Magnus' green salt. This result is in agreement with the low electrical conductivity ($<10^{-10}$ S/cm) in the alkyl-substituted complexes. Because the Pt−Pt interactions in the $[Pt(NH_2R)_4][PtCl_4]$ compounds are presumably weak, these substances may be regarded as self-assembled supramolecular structures. Nonetheless, the prepared complexes show some characteristics of rigid-rod polymers with flexible side chains; for example, they are insoluble when the alkyl chains are short but become soluble for longer alkyl chains, and they are able to form two-dimensional hexagonal or sheet structures. The complexes melt under decomposition above 100 °C. The soluble $[Pt(NH_2R)_4][PtCl_4]$ complexes form gels with fibrillar structures at temperature ranges that depend on the length of R. Films and fibers with uniaxially oriented fibrils were prepared from gels by drawing and electrostatic spinning. The mixed-metal complexes $[Pd(NH_2R)_4][PtCl_4]$ and $[Pt(NH_2R)_4][PdCl_4]$ (R = octyl) were also synthesized. The chemical and physical properties of the compounds with palladium differed significantly from those of $[Pt(NH_2R)_4][PtCl_4]$. In particular, one of these complexes is insoluble, whereas the other one decomposes relatively quickly in solution.

Introduction

Platinum (Pt) and palladium (Pd) complexes of the type $[M(NH_2R)_4][MCl_4]$ could be of interest in materials science as they can be regarded as rare examples of rigid-rod polymers or self-assembled supramolecular structures with a metallic main chain. However, the related complexes known so far are largely insoluble, in particular in organic solvents. These unfavorable properties are typical for rigid-rod polymers and often severely restrict or even prevent potential application. Increased processability may be achieved by introduction of flexible side chains attached to the rigid backbone. Although $[Pt(NH_2Bu)_4][PtCl_4]$ (Bu = butyl), which is the complex with the longest alkyl chains characterized so far, is still insoluble in organic solvents (and water), we expect that a further increase in chain length will increase the solubility. Thus, this study explores the synthesis, characterization, and properties of compounds of the type $[Pt(NH_2R)_4][PtCl_4]$, where R is an alkyl chain containing up to 14 carbon atoms. These complexes are also compared with related complexes with Pd as well as to Magnus' pink salt. Numerous, often confusing or conflicting reports exist in the literature, so this paper sets out with a (critical) historical background on related complexes.

Historical Background. Complexes of the type $[M(NH_3)_4][MCl_4]$, where M is Pd or Pt, have been known for almost 200 years. They appear to have been first described by Vauquelin for M = Pd in 1813,[1] where pink needles (Vauquelin's salt) were obtained immediately after addition of ammonia to an acidic solution of Pd salts (nitrates and chlorides). A number of articles referred to those experiments in the following years.[2−5] Although analysis of the pink needles revealed only ≈40% w/w of metallic Pd after heating in the open fire (expected 50% w/w) and the content of ammonia and chloride was not determined,[1] they are nowadays attributed to be $[Pd(NH_3)_4][PdCl_4]$ because of their method of preparation and appearance. The analytical difference with the early report might be explained by evaporation of volatile Pd compounds, as observed for corresponding Pt compounds analyzed later in a similar way.[6] Oddly, Vauquelin's salt is missing in the alphabetical list of all analyzed compounds known in 1819,[7] and we found

(1) Vauquelin *Ann. Chim.* **1813**, *88*, 167.
(2) Vauquelin *Ann. Philos.* **1814**, *4*, 216.
(3) Vauquelin *Ann. Philos.* **1814**, *4*, 271.
(4) Vauquelin; Hildebrandt *Schweigg. J.* **1814**, *12*, 265.
(5) Baruel *Quarterly J.* **1822**, *12*, 246.
(6) Gros, J. *Ann. Pharm.* **1838**, *27*, 241.
(7) Berzelius; Loewenhielm *Schweigg. J.* **1819**, *27*, 113.

10.1021/cm9806376 CCC: $18.00
Published on Web 02/27/1999

a complete and correct analysis published only in 1841.[8]

$[Pt(NH_3)_4][PtCl_4]$ was first prepared (and correctly analyzed) in 1828 by Magnus,[9] although a number of complexes consisting of Pt, Cl, and NH_3 had been described already between, for example, 1780 and 1820.[1,10−13] However, from their way of synthesis (typically based on the dissolution of elemental Pt in HNO_3/HCl) and their properties (color, solubility, analytical results) we conclude that they typically consisted of platinum(IV) complexes. Magnus, however, dissolved platinum(II) chloride in hydrochloric acid and added ammonia whereupon green crystals (Magnus' green salt) precipitated after some time.[9] In the following decades, several recipes were described to obtain Magnus' green salt from $PtCl_2$ and ammonia,[6,14] $K_2[PtCl_4]$ and ammonia,[15−17] $PtCl_2$ and $[Pt(NH_3)_4]Cl_2$,[18] $K_2[PtCl_4]$ and $[Pt(NH_3)_4]Cl_2$,[19−22] $(NH_3)_2[PtCl_4]$ and $[Pt(NH_3)_4]Cl_2$,[23] or by procedures with platinum(IV) complexes as educts.[24]

Structure of $[M(NH_3)_4][MCl_4]$ Complexes. The structure of Magnus' green salt was eventually elucidated with X-ray diffraction, revealing a linear arrangement of Pt chains with a Pt−Pt distance between 3.23 and 3.25 Å,[16,25,26] which is clearly above the typical Pt−Pt bond length of 2.6−2.8 Å.[27−34] It was suggested that the structure of Magnus' green salt is determined by electrostatic interactions rather than metal−metal bonds,[35,36] although some Pt−Pt interactions involving the $6p_z$ atomic orbitals are thought to be still present at distances of 4.0 Å.[35] The Coulomb lattice energy in Magnus' green salt is roughly −2000 kJ/mol.[36] As a result of its anisotropic structure, Magnus' green salt shows dichroism, which attracted attention in the past decades,[16−19,36,37] along with its electrical conductivity.[21,38−46] In addition to the homonuclear complexes, the mixed metal complexes $[Pt(NH_3)_4][PdCl_4]$ and $[Pd(NH_3)_4][PtCl_4]$ are known.[16,36] These substances exhibit a pink color[47] and, like $[Pd(NH_3)_4][PdCl_4]$, are isostructural with Magnus' green salt.[36,47] The Pt−Pd distance in $[Pt(NH_3)_4][PdCl_4]$ is 3.23,[16] and in $[Pd(NH_3)_4][PtCl_4]$ is 3.25,[16,25] and the Pd−Pd distance in $[Pd(NH_3)_4][PdCl_4]$ is 3.25 Å.[16]

Magnus' Pink Salt. Occasionally, a pink or red isomer of Magnus' green salt is also mentioned, usually designated as Magnus' pink salt. The precipitation of red Pt complexes from solutions containing Pt, ammonia (or ammonium), and chloride was described in great detail, e.g., already in 1782[10] and 1804,[12] but these complexes probably consisted of platinum(IV) complexes. In contrast, Magnus observed a red compound after treatment of platinum(II) chloride with NH_4Cl, which was, however, not analyzed.[9] Some authors[48,49] ascribed the first synthesis of a red isomer of Magnus' green salt to Vauquelin in 1817,[50,51] but we failed to find evidence for such a compound in the cited reports. We attribute most of the related substances to platinum(IV) complexes. The red prismatic crystals that were observed with platinum(II) chloride as an educt and that presumably contain Pt, chloride and ammonia[50] were not analyzed (the yield was too low) and were very soluble in water, which is not in agreement with the properties of Magnus' pink salt. Red or reddish complexes prepared with platinum(II) compounds as educts were described between 1844 and 1846.[48,52,53] They were attributed to compounds of the composition "$PtCl_3(NH_3)$" (note that we have already transformed the formula in the original literature into the terms presently used)[52,54] or to "$PtCl_2(NH_3)_2$",[48,53] that is, only the latter could consist of an isomer of Magnus' green salt, whereas the former might represent $(NH_4)_2[Cl_2Pt(\mu\text{-}Cl)_2PtCl_2]$, a compound of slightly different stoichiometry than "$PtCl_3(NH_3)$". A red intermediate appearing during the preparation of Magnus' green salt was mentioned in 1856,[55] but not analyzed. In 1906, the discovery of a red

(8) Fehling, H. *Ann. Chem. Pharm.* **1841**, *39*, 110.
(9) Magnus, G. *Pogg. Ann.* **1828**, *14*, 239.
(10) Bergmann, T. *Neuest. Entdeck. Chem.* **1782**, *4*, 120.
(11) Bergman, T. *Opuscules Chymiques et Physiques*, Vol. 2; Frantin: Dijon, 1785.
(12) Collet-Descotils, H. V. *J. Mines* **1804**, *15*, 46.
(13) Kels, H. W. *Handbuch der Chemie*; Stettinsche Buchhandlung: Ulm, 1791.
(14) Reiset, J. *Compt. Rend. Acad. Sci.* **1840**, *10*, 870.
(15) Clarke, F. W.; Owens, M. E. *Am. Chem. J.* **1881**, *3*, 350.
(16) Rodgers, M. L.; Martin, D. S. *Polyhedron* **1987**, *6*, 225.
(17) Martin, Jr., D. S.; Rush, R. M.; Kroening, R. F.; Fanwick, P. E. *Inorg. Chem.* **1973**, *12*, 301.
(18) Peyrone, M. *Ann. Chem. Pharm.* **1844**, *51*, 1.
(19) Yamada, S. *J. Am. Chem. Soc.* **1951**, *73*, 1579.
(20) Houlding, V. H.; Frank, A. J. *Inorg. Chem.* **1985**, *24*, 3664.
(21) Honda, K.; Chiba, K.; Tsuchida, E.; Frank, A. J. *J. Mater. Sci. Lett.* **1989**, *24*, 4004.
(22) Palkin, V. A.; Kuzina, T. A.; Kuz'mina, N. N.; Shchelokov, R. N. *Zh. Neorg. Khim.* **1980**, *25*, 1291; Engl. transl. *Russ. J. Inorg. Chem.* **1980**, *25*, 720.
(23) Palkin, V. A.; Kuz'mina, N. N.; Chernyaev, I. I. *Zh. Neorg. Khim.* **1965**, *10*, 41; Engl. transl. *Russ. J. Inorg. Chem.* **1965**, *10*, 23.
(24) Grube, H.-L. In *Handbuch der Präparativen Anorganischen Chemie*; Brauer, G., Ed.; Ferdinand Enke: Stuttgart, 1981; p 1704.
(25) Miller, J. R. *J. Chem. Soc.* **1965**, 713.
(26) Atoji, M.; Richardson, J. W.; Rundle, R. E. *J. Am. Chem. Soc.* **1957**, *79*, 3017.
(27) Yoshida, T.; Yamagata, T.; Tulip, T. H.; Ibers, J. A.; Otsuka, S. *J. Am. Chem. Soc.* **1978**, *100*, 1064.
(28) Braunstein, P.; Jud, J.-M.; Dusausoy, Y.; Fischer, J. *Organometallics* **1983**, *2*, 180.
(29) Frew, A. A.; Hill, R. H.; Manojilovic-Muir, L.; Muir, K. W.; Puddephatt, R. J. *J. Chem. Soc., Chem. Commun.* **1982**, 198.
(30) Goodfellow, R. J.; Herbert, I. R.; Orpen, A. G. *J. Chem. Soc., Chem. Commun.* **1983**, 1386.
(31) Brown, M. P.; Puddephatt, R. J.; Rashidi, M.; Manojlovic-Muir, L.; Muir, K. W.; Solomun, T.; Seddon, K. R. *Inorg. Chim. Acta* **1977**, *23*, L33.
(32) Ciriano, M.; Howard, J. A. K.; Spencer, J. L.; Stone, F. G. A.; Wadepohl, H. *J. Chem. Soc., Dalton Trans.* **1979**, 1749.
(33) Modinos, A.; Woodward, P. *J. Chem. Soc., Dalton Trans.* **1975**, 1516.
(34) Taylor, N. J.; Chieh, P. C.; Carty, A. J. *J. Chem. Soc., Chem. Commun.* **1975**, 448.
(35) Interrante, L. V.; Messmer, R. P. *Inorg. Chem.* **1971**, *10*, 1175.
(36) Miller, J. R. *J. Chem. Soc.* **1961**, 4452.
(37) Anex, B. G.; Ross, M. E.; Hedgcock, M. W. *J. Chem. Phys.* **1967**, *46*, 1090.
(38) Summa, G. M.; Scott, B. A. *Inorg. Chem.* **1980**, *19*, 1079.
(39) Rao, C. N. R.; Bhat, S. N. *Inorg. Nucl. Chem. Lett.* **1969**, *5*, 531.
(40) Interrante, L. V. *J. Chem. Soc, Chem. Commun.* **1972**, 302.
(41) Gomm, P. S.; Thomas, T. W.; Underhill, A. E. *J. Chem. Soc. A* **1971**, 2154.
(42) Mehran, F.; Scott, B. A. *Phys. Rev. Lett.* **1973**, *31*, 99.
(43) Interrante, L. V. *Adv. Chem. Ser.* **1976**, *150*, 1.
(44) Mehran, F.; Interrante, L. V. *Solid State Commun.* **1976**, *18*, 1031.
(45) Kubota, R.; Kobayashi, H.; Tsujikawa, I.; Enoki, T. *Int. J. Quantum Rev.* **1980**, *18*, 1533.
(46) Tanaka, M.; Kojima, N.; Ajiro, Y.; Ban, T.; Tsujikawa, I. *Synth. Met.* **1987**, *19*, 967.
(47) Miller, J. R. *Proc. Chem. Soc.* **1960**, 318.
(48) Peyrone, D.-M. *Ann. Chim. Phys., Sér. 3* **1846**, *16*, 462.
(49) Wittstein, G. C. *Repertorium Pharm.* **1848**, *100*, 456.
(50) Vauquelin *Ann. Chim. Sér. 2* **1817**, *5*, 260.
(51) Vauquelin *Ann. Chim. Sér. 2* **1817**, *5*, 392.
(52) Reiset, J. *Compt. Rend. Acad. Sci.* **1844**, *18*, 1100.
(53) Peyrone, M. *Ann. Chem. Pharm.* **1845**, *55*, 205.
(54) Reiset, J. *Ann. Chim. Phys. Sér. 3* **1844**, *11*, 417.
(55) Grimm, C. *Ann. Chem. Pharm.* **1856**, *99*, 95.

modification of Magnus' green salt was ascribed to a student called Bjerrum, and it was deduced by chemical reactions that this red salt was composed of $[Pt(NH_3)_4]^{2+}$ and $[PtCl_4]^{2-}$ units.[56] It was also suggested that Magnus' pink salt consists mainly of $[Pt(NH_3)_3Cl]_2[PtCl_4]$,[57] but other authors strongly disagreed because the properties of Magnus' pink salt and $[Pt(NH_3)_3Cl]_2[PtCl_4]$ are completely different.[58] Finally, it was reported that it is difficult to obtain the pink modification in absence of the green modification.[23] Magnus' pink salt with a minor fraction of the green version (estimated to 1−3%) was obtained from $(NH_3)_2[PtCl_4]$ and $[Pt(NH_3)_4]Cl_2$.[23] It was not possible to get crystals of Magnus' pink salt suited for single-crystal X-ray diffraction (XRD);[26,59] however, from powder diffraction patterns it was concluded that the Pt−Pt distance in the salt is >5 Å.[26]

Alkyl-Substituted Complexes. Green and pink complexes of the type $[M(NH_2R)_4][MCl_4]$, where R is an alkyl group, have also been reported. The compound with R = methyl is green[36,47,56,60−63] and isostructural with Magnus' green salt[47] (Pt−Pt distance of 3.25 Å[16,25] or 3.29 Å[62]). A brown-yellow[60] and a pink (or red)[36,61,62,64] modification was described for R = ethyl. Single crystals suited for X-ray analysis of the pink complex apparently were extremely difficult to obtain, but the structure could be solved, revealing linearly arranged Pt atoms separated by 3.62 Å.[62] The plane of the Pt−N coordination square is inclined by 29° to that of the tetrachloroplatinate(II) plane.[62] A pink or red modification for R = butyl and propyl was also described,[61,64] but the Pt analysis for R = propyl in one of those reports[64] is not correct (the calculated Pt content, 58.78%, is inconsistent with the expected composition). The green complex with R = methyl[61,64] and the pink with R = ethyl[61] and butyl[64] show a dichroic behavior. Greenish-grey modifications for R = butyl, propyl, and 2-methylpropyl were also mentioned but not analyzed, nor were properties of those substances described.[63] Reports on a brown modification with R = ethyl and a green with 1-aminobutane[65] are inconsistent because the analyzed Pt contents clearly disagree with the expected values (note that the calculated Pt contents,[65] 40.76 for R = 1−aminoethane and 45.5% for R = 1-aminobutane, are incorrect), which was obviously not recognized when cited by Jörgensen.[64] Finally, it was suggested, but not shown, that 1-aminoalkanes with two or more carbon atoms should give rise only to the formation of pink isomers since the packing of the alkyl groups increases the Pt−Pt distance compared with that in Magnus' green salt;[61] however, an increasing number of carbon atoms would not necessarily prevent the Pt atoms from approaching each other as closely as required for the formation of the green isomer.[61]

Experimental Section

General. All chemical educts and solvents were obtained from commercial sources (Fluka, Aldrich, Johnson Matthew) and used as received. For ultraviolet (UV) measurements in chloroform, UV grade was used (Fluka).

The elemental analyses of carbon, hydrogen, nitrogen, and chlorine were performed by the microelemental service of the Laboratorium für Organische Chemie at ETH Zürich. Noble metal analyses were performed by the analytical service of the Laboratorium für Anorganische Chemie at ETH Zürich.

Thermogravimetric analysis (TGA) and differential scanning calorimetry (DSC) were performed with equipment from Netzsch (TG 209 and DSC 200, respectively) under nitrogen atmosphere at heating rates of 10 °C/min if not otherwise indicated. Infrared (IR) spectra were recorded with CsCl pellets on a Bruker IFS 66v spectrometer. For optical microscopy, a Leica DMRX microscope equipped with two polarizers and a Mettler Toledo FP82 HT hot stage was used. X-ray photoelectron spectroscopy (XPS) was performed as described elsewhere.[66]

Near-edge X-ray absorption fine structure spectroscopy (NEXAFS) experiments were performed on Exxon beamline U1A at the National Synchrotron Light Source (NSLS), Brookhaven National Laboratory, New York, in the partial electron yield mode for normal and grazing incidence of the X-rays. All spectra were normalized to the incoming photon flux by division by simultaneously recorded spectra from a gold-covered reference grid. In addition, the spectra were normalized to the ionization step.[67] To account for the severe charging of the samples, a floodgun was used.[68]

Small-angle X-ray scattering (SAXS) patterns were obtained from dried gels of the respective complexes on a Kiessig small-angle-scattering camera, equipped with a Seifert ISO-Debyeflex 2002 polaroid cassette, using Ni-filtered Cu Kα radiation (wavelength 1.5416 Å). Because the spacings of the (100) reflections could be determined only with limited precision (at very low angles), they were calculated from the (200) reflections that could be measured more accurately.

Transmission electron microscopy (TEM) was performed with a Philips CM12 electron microscope equipped with a precooled cold stage (MIDILAB) using a dry nitrogen counterflow loading device. The samples were kept in the MIDILAB unit for 2 h at −80 °C at a pressure of $<10^{-7}$ mbar, transferred to a specially designed Gatan cryoholder, and examined at an acceleration voltage of 100 kV below −175 °C. Images were recorded with a Gatan 694 slow scan charge-coupled device (CCD) camera at a low electron flux ($0.5e^-/Å^2$).

Electrostatic spinning was executed at room temperature with a simple laboratory spinning apparatus[69] using a gel of tetrakis(1-aminooctane)platinum(II) tetrachloroplatinate(II) in toluene at a concentration of 40 mg/mL. For the spinning process, a voltage of 10 000 V was applied. The distance between the electrodes was 20 cm and the jet diameter 1 mm.

Syntheses. In the following syntheses, filtrations were performed with sintered-glass funnels (type N4, diameter 2, 4, or 6 cm) if not otherwise indicated. The products were dried at 10^{-2} mbar for 24 h if not otherwise indicated.

Magnus' Pink Salt. First, 972.8 mg of $K_2[PtCl_4]$ were dissolved in 20 mL of water and heated to 60 °C. Then, 7 mL of 25% ammonia solution were added, and a yellow-brown precipitate formed immediately. The mixture was stirred at 60 °C for 1 h. Next, the suspension was heated to boiling until the solid was completely dissolved. The colorless solution was then cooled with ice to 0 °C and joined with a solution of 973.1 mg of $K_2[PtCl_4]$ in 20 mL water that had also been cooled with ice. A pink precipitate formed immediately which was instantaneously filtered and washed in the funnel with 50 mL of ice

(56) Jörgensen, S. M.; Sörensen, S. P. L. *Z. Anorg. Chem.* **1906**, *48*, 441.
(57) Cox, E. G.; Pinkard, F. W.; Wardlaw, W.; Preston, G. H. *J. Chem. Soc.* **1932**, 2527.
(58) Drew, H. D. K.; Tress, H. J. *J. Chem. Soc.* **1935**, 1586.
(59) Hertel, E.; Schneider, K. *Z. Anorg. Allg. Chem.* **1931**, *202*, 77.
(60) Wurtz, A. *Ann. Chim. Phys. Sér. 3* **1850**, *30*, 443.
(61) Yamada, S.; Tsuchida, R. *Bull. Chem. Soc. Jpn.* **1958**, *31*, 813.
(62) Cradwick, M. E.; Hall, D.; Phillips, R. K. *Acta Crystallogr. B* **1971**, *27*, 480.
(63) Tschugaeff, L. *Ber. Deutsch. Chem. Ges.* **1907**, *40*, 173.
(64) Jörgensen, S. M. *J. Prakt. Chem.* **1886**, *141*, 488.
(65) Gordon, C. *Ber. Deutsch. Chem. Ges.* **1870**, *3*, 174.
(66) Fischer, D.; Caseri, W. R.; Hähner, G. *J. Colloid Interface Sci.* **1998**, *198*, 337.
(67) Stöhr, J. *NEXAFS Spectroscopy*; Springer: Heidelberg, 1992.
(68) Hähner, G.; Marti, A.; Spencer, N. D.; Caseri, W. R. *J. Chem. Phys.* **1996**, *104*, 7749.
(69) Baumgarten, P. K. *J. Colloid Interface Sci.* **1971**, *36*, 71.

Table 1. Calculated and Found Chemical Composition (in % w/w) of the Compounds of the Formula $[M^1(NH_2R)_4][M^2Cl_4]$, with R = H or Alkyl

M^1	M^2	R		C	H	N	Cl
Pt	Pt	H (pink salt)	found		1.95	9.31	23.49
			calc		2.02	9.34	23.63
		H (green salt)	found		2.21	9.19	23.68
			calc		2.02	9.34	23.63
		$(CH_2)_3CH_3$	found	23.16	5.14	6.70	17.32
			calc	23.31	5.38	6.80	17.20
		$(CH_2)_6CH_3$	found	34.15	6.68	5.78	14.30
			calc	33.87	6.90	5.64	14.28
		$(CH_2)_7CH_3$	found	36.63	7.10	5.31	13.34
			calc	36.64	7.30	5.34	13.52
		$(CH_2)_8CH_3$	found	39.11	7.49	5.08	12.62
			calc	39.13	7.66	5.07	12.83
		$(CH_2)_9CH_3$	found	41.41	7.72	4.79	12.01
			calc	41.38	7.99	4.83	12.21
		$(CH_2)_{11}CH_3$	found	45.48	8.60	4.38	11.26
			calc	45.28	8.55	4.40	11.14
		$(CH_2)_{13}CH_3$	found	48.79	9.00	4.03	9.99
			calc	48.54	9.02	4.04	10.23
Pt	Pd	$(CH_2)_7CH_3$	found	39.82	7.91	5.72	14.80
			calc	40.02	7.98	5.83	14.77
Pd	Pt	$(CH_2)_7CH_3$	found	39.74	7.75	5.93	15.07
			calc	40.02	7.98	5.83	14.77

water and 40 mL of ethanol, and dried (yield 75%). Elemental analyses are presented in Table 1.

Magnus' Green Salt. First, 156 mg of Magnus' pink salt were poured into 25 mL of water, and the suspension was kept in a round-bottomed flask equipped with a reflux condenser at the boiling temperature for 2 h, resulting in a dark, green-grey solid. A solution of 19 mL of concentrated hydrochloric acid (37% w/w) and 73 mL of water was added to the reaction mixture, whereupon the color of the solid turned to green. The mixture was heated until the solid dissolved. The yellow solution was filtered through a cellulose filter (Schleicher & Schuell, Feldmeilen, Switzerland), and the filtrate was kept at 0 °C overnight. During this period, 87 mg (yield 56%) of green crystals precipitated that were filtered and dried. Elemental analyses are presented in Table 1.

Tetrakis(1-aminobutane)platinum(II) Tetrachloroplatinate(II). A solution of 1.0 g (2.4 mmol) of $K_2[PtCl_4]$ in 20 mL of water was treated at 60 °C with 4.7 mL (47 mmol) of 1-aminobutane and stirred. A white solid precipitated after ≈5 min and dissolved after ≈20 min. After 1 h at 60 °C, the solution was allowed to cool to room temperature and, upon addition of 1.0 g (2.4 mmol) of $K_2[PtCl_4]$ dissolved in 20 mL of water, the product precipitated quickly. Immediately, 100 mL of hexane were added, and the mixture was instantly filtered and washed in the funnel with 50 mL of hexane, and dried (yield 80%). Elemental analyses are presented in Table 1.

$[Pt\{NH_2(C_nH_{2n+1})\}_4][PtCl_4]$, $n = 7-12$. A solution of 1.0 g (2.4 mmol) of $K_2[PtCl_4]$ in 20 mL of water was heated to 60 °C. An excess of the amine (47 mmol) was added, and the solution (two phases) was stirred at 60 °C. A white solid precipitated after ≈5 min and dissolved after ≈20 min. After 1 h at 60 °C, the reaction mixture, which consisted of a yellow organic phase and an opaque aqueous phase, was allowed to cool to room temperature. Thereafter, another 1.0 g (2.4 mmol) of $K_2[PtCl_4]$ in 20 mL of water was added, and a precipitate formed rapidly. Immediately, 100 mL of hexane were mixed into the suspension, and the mixture was instantly filtered, washed in the funnel with 50 mL of hexane, and dried. The pink solid was recrystallized by pouring into 50 mL of $CHCl_3$, followed by heating the mixture to 60 °C in a round-bottomed flask equipped with a reflux condenser. After 20 min, the solution was cooled to room temperature and filtered through a Teflon filter (pore diameter, 1 μm). The product was precipitated by addition of 50 mL ethanol to the filtrate. The suspension was filtered, washed in the funnel with 20 mL of ethanol, and dried. The following yields were obtained: $n = 7$, 78%; $n = 8$, 73%; $n = 9$, 84%; $n = 10$, 54%; $n = 12$, 64%. Elemental analyses are presented in Table 1. For $n = 8$, the ratio Pt:N:Cl was confirmed by XPS (1:2:2). The Pt analysis for $n = 12$ gave 30.9% Pt (calculated 30.6%).

Tetrakis(1-aminotetradecane)platinum(II) Tetrachloroplatinate(II). A solution of 1.0 g (2.4 mmol) of $K_2[PtCl_4]$ in 20 mL of water and 8 mL of ethanol was heated to 60 °C. Then, 10.0 g (47 mmol) of 1-aminotetradecane were added, and the mixture was stirred at 60 °C. A white solid precipitated after ≈5 min and then dissolved within hours. After 16 h at 60 °C, the reaction mixture consisted of a yellow organic phase and an opaque aqueous phase. This mixture was cooled to room temperature and 1.0 g (2.4 mmol) of $K_2[PtCl_4]$ in 20 mL of water and 8 mL of ethanol were added. A solid precipitated rapidly, and immediately 100 mL of hexane were poured into the suspension. The mixture was instantly filtered through a sintered-glass funnel and washed in the funnel with 50 mL of hexane. The product was dried and afterward suspended in 50 mL of $CHCl_3$. Upon heating to 60 °C in a round-bottomed flask equipped with a reflux condenser for 20 min, the solid dissolved. The solution was cooled to room temperature and filtered through a Teflon filter (pore diameter 1 μm). Addition of 50 mL of ethanol to the filtrate resulted in the precipitation of the desired compound. The suspension was filtered, washed in the funnel with 20 mL of ethanol, and dried (yield 81%). Elemental analyses are presented in Table 1. In addition, a Pt content of 28.3% (calculated 28.2%) was found.

Tetrakis(1-aminooctane)platinum(II) Dichloride. First, 5.309 g (12.8 mmol) of $K_2[PtCl_4]$ were dissolved in 100 mL of water. The solution was stirred and heated to 60 °C. Thereafter, 40 mL (242 mmol) of 1-aminooctane were added. A white-yellow precipitate formed that dissolved after ≈30 min of stirring. The reaction mixture consisted of a yellow organic phase and an opaque aqueous phase. After 1 h at 60 °C, the reaction mixture was reduced to ≈65% of its volume with a rotary evaporator at 50 °C and 60 mbar. A white, shiny precipitate formed that was filtered through a sintered-glass funnel, washed in the funnel with 50 mL of water and thereafter with 150 mL of hexane, and dried. An additional amount of the desired product was obtained after reduction of the filtrate to ≈30% of its volume with a rotary evaporator at 50 °C and 60 mbar followed by cooling of the liquid with ice. Again, a white solid precipitated that was washed with water and hexane and dried as already described. The yield was 81%, and the following elemental contents were found (in % w/w, calculated values in parentheses): C 49.23 (49.09), H 9.28 (9.78), N 7.08 (7.16), Cl 9.01 (9.06).

Tetrakis(1-aminooctane)palladium(II) Dichloride. A solution of 300 mg (0.9 mmol) of $K_2[PdCl_4]$ in 10 mL of water was heated to 60 °C and treated with 2.6 mL (16 mmol) of 1-aminooctane. Immediately, a yellow precipitate formed that rapidly dissolved. After 30 min at 60 °C, the reaction solution consisted of a yellow organic phase and an opaque aqueous phase. After 1 h, the reaction mixture was cooled to room temperature. Then, the solution was concentrated to ≈10 mL at 75−100 mbar using a rotary evaporator. A white, shiny solid precipitated that was filtered and washed first with 20 mL of water and then with 50 mL of hexane in the funnel, and the white powder was dried (yield 71%). The following elemental contents were found (in % w/w, calculated values in parentheses): C 55.37 (55.36), H 10.99 (11.03), N 8.01 (8.07), Cl 10.09 (10.21).

Tetrakis(1-aminooctane)platinum(II) Tetrachloropalladate(II). First, 300 mg (0.38 mmol) of $[Pt\{NH_2(CH_2)_7CH_3\}_4]Cl_2$ were dissolved in 10 mL of chloroform. This solution was mixed with a solution of 126 mg (0.39 mmol) of $K_2[PdCl_4]$ in 20 mL of water and 60 mL of ethanol that was previously cooled with ice. A red-brown precipitate and two liquid phases formed instantly. The liquid phases were an organic phase that contained the precipitate and an opaque aqueous phase. The mixture was shaken and the aqueous phase separated and was discarded. The organic phase was filtered, and the remaining pink product was dried (yield 91%). The content of analyzed elements is given in Table 1. The ratio Pt:Pd:N:Cl was confirmed by XPS (1:1:4:4).

Tetrakis(1-aminooctane)palladium(II) Tetrachloroplatinate(II). A solution of 200 mg (0.61 mmol) of $K_2[PdCl_4]$

in 5 mL of water was heated to 60 °C. An excess of 1-aminoalkane (2.0 mL, 12 mmol) was added, and immediately an orange-brown precipitate formed and then dissolved rapidly. The solution was kept at 60 °C for 30 min. The liquid consisted of a yellow organic phase and an opaque aqueous phase. After cooling to room temperature, 254 mg (0.61 mmol) of $K_2[PtCl_4]$ in 5 mL of water were added, whereupon a pink solid precipitated instantly. Immediately, 20 mL of hexane were mixed into the solution, and the suspension was filtered, washed with 20 mL of hexane in the funnel, and finally dried. The pink product was recrystallized by dissolving in 20 mL of chloroform at 60 °C. Immediately after its dissolution, the liquid was rapidly filtered through a Teflon filter (pore diameter 1 μm). Instantly, 20 mL of ethanol were added to the filtrate and a pink solid precipitated immediately. The precipitation was immediately filtered, washed with 20 mL of ethanol in the funnel, and finally dried (yield 68%). The content of analyzed elements is given in Table 1. The ratio Pd:Pt:N:Cl was confirmed by XPS (1:1:4:4).

Attempt at Preparation of Tetrakis(1-aminooctane)-palladium(II) Tetrachloropalladate(II). First, 200.0 mg (0.29 mmol) of $[Pd\{NH_2(CH_2)_7CH_3\}_4]Cl_2$ were dissolved in 5 mL of ethanol and mixed with a solution of 94.1 mg (0.29 mmol) of $K_2[PdCl_4]$ in 5 mL of water. Immediately, a yellow solid precipitated, which was instantly filtered with a sintered-glass funnel, washed first with 20 mL of water and then with 20 mL of ethanol in the funnel, and finally dried. The yield was 74%. This precipitate was referred to as "$C_{16}H_{36}N_2Cl_2Pd$", and the following elemental contents were found (in % w/w, calculated values in parentheses): C 44.83 (44.10), H 8.54 (8.79), N 6.57 (6.43), Cl 16.48 (16.27).

Preparation of Crystals of *trans*-bis(1-Aminooctane)-dichloroplatinum(II). First, 1.29 g (2.7 mmol) of *cis*-dichlorobis(styrene)platinum(II), which was prepared according to the literature,[70] were dissolved in 45 mL of chloroform. The solution was heated to 60 °C and mixed with 0.9 mL (5.4 mmol) of 1-aminooctane. The yellow solution was kept at 60 °C for 1 h. Thereafter, the solvent was removed completely with a rotary evaporator at 400 mbar. The yellow-white powder was dried at 10^{-2} mbar for 16 h. Chloroform was added to the solid until the powder was dissolved, and a gray substance was precipitated by pouring 50 mL of hexane into the solution. The gray substance was separated from the liquid by filtration, and the filtrate was concentrated at 400 mbar to ≈30% with a rotary evaporator. The solution was stored at 5 °C for 20 h, whereupon crystals formed that were filtered, washed with 50 mL of hexane in the funnel, and dried. The yield of crystals, suited for XRD (see *Appendix*), was 16%, and the following elemental contents were found (in % w/w, calculated values in brackets): C 36.53 (36.64), H 7.02 (7.30), N 5.28 (5.34), Cl 13.54 (13.52).

Results

Magnus' Pink Salt. We synthesized Magnus' pink salt with $K_2[PtCl_4]$ and in-situ-prepared $[Pt(NH_3)_4]^{2+}$ at 0 °C. The detailed procedure and the elemental analyses are given in the *Experimental Section*. We observed that it was important to keep the temperature low during the synthesis because otherwise an increasing amount of Magnus' green salt was formed.

Magnus' pink salt was investigated with XPS and IR spectroscopy. The results obtained from XPS are presented later in the context of the mixed-metal complexes. Table 2 presents IR frequencies of Magnus' pink salt, which to our knowledge have not yet been reported. These frequencies are compared with those of Magnus' green salt (prepared from Magnus' pink salt, see *Experimental Section*), $[Pt(NH_3)_4]Cl_2$, $K_2[PtCl_4]$, *cis*-$[Pt(NH_3)_2Cl_2]$, *trans*-$[Pt(NH_3)_2Cl_2]$, and $[Pt(NH_3)_3Cl]^+$. The attribution of the frequencies to the related vibrations in Table 2 is based on detailed discussions of previously reported IR spectra of Magnus' green salt,[71,72] $[Pt(NH_3)_4]Cl_2$,[73,74] and $K_2[PtCl_4]$,[75] all of which we recorded again and found to be in full agreement with those reported in the literature.

Table 2. IR Frequencies (in cm^{-1}) of Pt(II) Amine Complexes and of Potassium Tetrachloroplatinate(II)

compound	ν(N−H)	δ(NH_3)	ρ(NH_3)	ν(Pt−N)	ν(Pt−Cl)
Magnus' pink salt	3269	1650	851	508	321
	3135	1540	829		
		1349			
		1329			
		1312			
Magnus' green salt	3274	1631	829	500	311
	3135	1580			
		1547			
		1312			
$[Pt(NH_3)_4]Cl_2$	3259	1576	894	510	
	3182	1327	846		
$K_2[PtCl_4]$					323
cis-$[PtCl_2(NH_3)_2]$[a]	—[b]	1625	795	510	330
		1544			323
		1316			
		1301			
trans-$[PtCl_2(NH_3)_2]$[a]	—[b]	1627	825	509	330
		1530	804		
		1290			
$[Pt(NH_3)_3Cl]^+$[c,d]	3308	1575	815	489	315
	3210	1327	785		

[a] Reference 72. [b] Frequency not reported. [c] Reference 74. [d] Counterion not reported.

The ν(N−H) in Magnus' pink salt are poorly resolved, in contrast to the related peaks in the spectrum of Magnus' green salt. The frequencies of the δ(NH_3) differ in Magnus' pink and green salts, and the related signals between 1540 and 1650 cm^{-1} are broad and hardly resolved in Magnus' pink salt, but sharp in the green isomer. Compared with Magnus' green salt, a new, broad and strong δ(NH_3) signal arises at 851 cm^{-1} in the pink salt, which may appear also in Magnus' green salt as a shoulder. Although the peak of ν(Pt−N) in Magnus' green salt is hardly visible, in agreement with the literature,[71] it is clearly visible in Magnus' pink salt. Finally, ν(Pt−Cl) differs by 10 cm^{-1} in Magnus' pink and green salt. As a whole, the IR spectra of Magnus' green and pink salts differ significantly, clearly indicating that the structures of these isomers are not identical.

In Magnus' pink salt, ν(Pt−Cl) matches with that of $K_2[PtCl_4]$, and ν(Pt−N) matches with that of $[Pt(NH_3)_4]Cl_2$. These results are consistent with the assumption that Magnus' pink salt contains $[PtCl_4]^{2-}$and $[Pt(NH_3)_4]^{2+}$ moieties in which Pt−Pt interactions are of minor relevance, in contrast to Magnus' green salt where ν(Pt−Cl) is shifted to lower frequencies related to $K_2[PtCl_4]$. Differences in the positions of ν(N−H) between Magnus' pink salt and $[Pt(NH_3)_4]Cl_2$ might be due to inter- or intramolecular interactions of N−H

(70) Albinati, A.; Caseri, W. R.; Pregosin, P. S. *Organometallics* **1987**, *6*, 788.

(71) Hall, J. R.; Hirons, D. A. *Inorg. Chim. Acta* **1979**, *34*, L277.
(72) Clark, R. J. H.; Williams, C. S. *J. Chem. Soc. A* **1966**, 1425.
(73) Shimanouchi, T.; Nakagawa, I. *Inorg. Chem.* **1964**, *3*, 1805.
(74) Hiraishi, J.; Nakagawa, I.; Shimanouchi, T. *Spectrochim. Acta A* **1968**, *24*, 819.
(75) Ferraro, J. R. *Low-Frequency Vibrations of Inorganic and Coordination Compounds*; Plenum Press: New York, 1971.

bonds (e.g., weak hydrogen bonds with chloride[76]) or to electrostatic interactions (see NEXAFS results later). The IR spectrum of Magnus' pink salt clearly differs from those of *cis*-$[Pt(NH_3)_2Cl_2]$, *trans*-$[Pt(NH_3)_2Cl_2]$ and $[Pt(NH_3)_3Cl]^+$ moieties (cf. Table 2), in particular the frequencies of $\delta(NH_3)$ and $\rho(NH_3)$. In addition, $[Pt(NH_3)_3Cl]^+$ shows a different $\nu(Pt-N)$ frequency. As mentioned in the *Introduction*, there has been some discussion in the literature whether or not Magnus' pink salt is identical to $[Pt(NH_3)_3Cl]_2[PtCl_4]$. According to the present IR spectra, we confirm the currently accepted opinion that ascribes Magnus' pink salt to a compound of the structure $[Pt(NH_3)_4][PtCl_4]$.[23,58]

It has been suggested[23] that Magnus' pink salt is always contaminated with Magnus' green salt. Although we could not detect $\nu(Pt-Cl)$ of Magnus' green salt in the spectrum of Magnus' pink salt, it may contain some of the green isomer; we estimate the detection limit in the IR spectra to be ≈10%. Hence, we cannot fully exclude that the signals at 830 and 1312 cm^{-1} in the IR spectrum of the pink powder, which are superimposed on the peaks at 851 and 1329 cm^{-1}, respectively, are caused by vibrations of Magnus' green salt. However, the content of Magnus' green salt in the pink modification can also be deduced by DSC. The DSC diagram of Magnus' green salt exhibits a strong endothermal transition at ≈320 °C (heating rate 10 °C/min), indicating the melting or decomposition of the substance. This transition could not be observed at all in the diagram of Magnus' pink salt, in which a content of a few weight percent of Magnus' green salt should be detectable.

$[Pt(NH_2R)_4][PtCl_4]$, Where R = Butyl, Heptyl, Octyl, Nonyl, Decyl, Dodecyl, or Tetradecyl. The compounds of the type $[Pt(NH_2R)_4][PtCl_4]$ reported so far (see *Introduction*), where R is an alkyl chain not longer than butyl, were prepared in aqueous solution from $K_2[PtCl_4]$ and $[Pt(NH_2R)_4]Cl_2$,[61] $K_2[PtCl_4]$ and the 1-aminoalkane,[16,64] or $PtCl_2$ and the 1-aminoalkane.[60] First, we prepared $[Pt(NH_2R)_4]^{2+}$ in situ from $[PtCl_4]^{2-}$ and an excess of the 1-aminoalkane and then we added a solution of tetrachloroplatinate(II), whereupon $[Pt(NH_2R)_4][PtCl_4]$ precipitated rapidly (as described in detail in the *Experimental Section*). The excess of 1-aminoalkane was removed after precipitation without delay, because otherwise the $[Pt(NH_2R)_4][PtCl_4]$ complexes began to decompose. The elemental analyses of the obtained pink solids agree well with the expected compositions (see *Experimental Section*).

As quoted in the *Introduction*, brown, green, and greenish-grey modifications of the compound with R = butyl were also mentioned in the literature.[63,65] We obtained solids of these colors when synthesis of $[Pt(NH_2R)_4][PtCl_4]$ was carried out at elevated temperatures or when pink complexes were heated to 130−140 °C. The chemical analyses of the brown products were not consistent with the expected composition. The greenish-grey products with R = butyl and longer chains showed good agreement with the elemental composition of $[Pt(NH_2R)_4][PtCl_4]$. However, their IR spectra were virtually indistinguishable from those of *trans*-$[PtCl_2(NH_2R)_2]$. Single crystals could be isolated from the greenish-grey solid for R = decyl and subjected to X-ray analysis, revealing *trans*-$[PtCl_2(NH_2R)_2]$ (see *Appendix*). We conclude that the greenish-grey products consist mainly of *trans*-$[PtCl_2(NH_2R)_2]$ and that the color of the solid is determined by impurities (*trans*-$[PtCl_2(NH_2R)_2]$ is yellow).

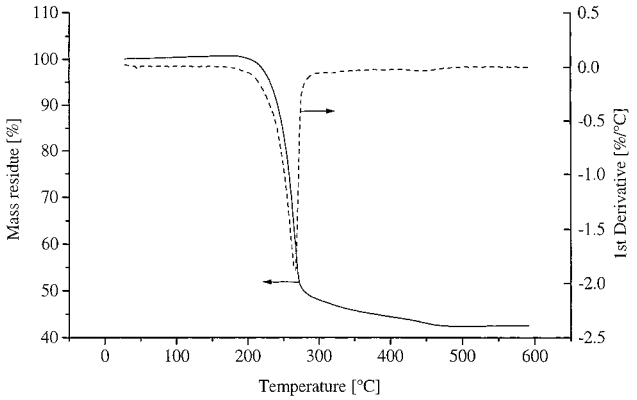

Figure 1. TGA plot of $[Pt(NH_2R)_4][PtCl_4]$, with R = octyl.

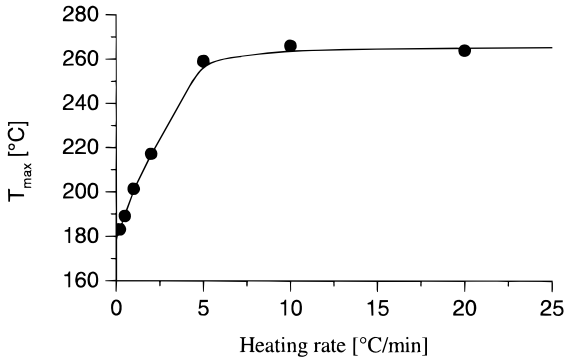

Figure 2. Temperature at maxiumum rate of weight loss (T_{max}) observed in TGA of $[Pt(NH_2R)_4][PtCl_4]$, with R = octyl, at different heating rates. The indicated line represents an empirical fit.

Thermogravimetric Analysis. All compounds of the type $[Pt(NH_2R)_4][PtCl_4]$ show similar behavior when subjected to TGA at a heating rate of 10 °C/min; an example is shown in Figure 1. Mass loss begins at ≈200 °C and reaches a maximum rate at ≈230 °C. Above ≈450 °C, the mass remains constant. In addition, the compound with R = octyl was measured at different heating rates between 0.2 and 20 °C/min. The temperature of maximum rate of mass loss decreases with decreasing heating rate (Figure 2), and the empirical extrapolation toward a heating rate of 0 °C/min resulted in a value of 179 °C. The marked dependence of those temperatures on the heating rates indicates that kinetic factors play an important role in the decomposition process. The temperature of initial perceptible mass loss is ≈130 °C for heating rates between 0.2 and 1.0 °C/min. After decompositon, the mass residue does not change within the experimental precision upon variation of the heating rate. The relative mass of this residue, when compared with the initial mass, depends linearly on the platinum content of the compounds (Figure 3). The mass of the residue is typically 7% above the mass of the initial Pt content, as reflected by the slope of the regression line of 1.07. It is most probable that the residue contains Pt compounds rather than, for example, graphite-like compounds, as in the latter case a

(76) Nakamoto, K. *Infrared Spectra of Inorganic and Coordination Compounds*; John Wiley: New York, 1970.

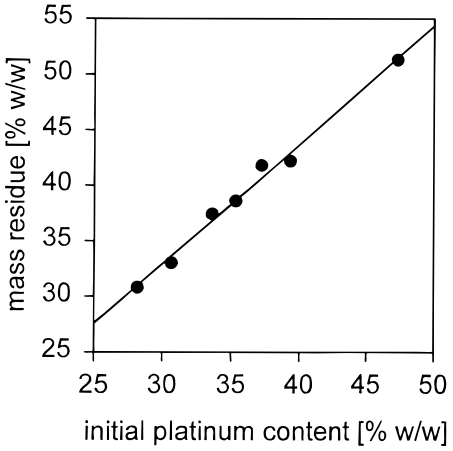

Figure 3. Mass residue of $[Pt(NH_2R)_4][PtCl_4]$ complexes after heating to 600 °C as a function of the initial platinum content.

Table 3. Irreversible DSC Transitions [°C] at a Heating Rate of 10 °C/min of Complexes of the Type $[Pt(NH_2R)_4][PtCl_4]$, $R=(CH_2)_nCH_3$

n	1st endothermal	exothermal	2nd endothermal
3	133	139	154
6	158	161	169
7	163	165	177
8	162	164	173
9	167	171	173
11	159	161	172
13	154	158	171

slope of <1 would be expected. The formation of volatile Pt compounds as observed upon heating Magnus' green salt in the open fire[6] could not be observed for $[Pt(NH_2R)_4][PtCl_4]$ complexes with the controlled heating procedure used here.

Differential Scanning Calorimetry Analysis. The DSC analyses, with a heating rate of 10 °C/min, of carefully recrystallized $[Pt(NH_2R)_4][PtCl_4]$ compounds were reproducible, manifesting in an unambiguous elemental analysis. The analyses show three irreversible transitions upon heating (Table 3). An example of a DSC thermogram is shown in Figure 4, where the step at ≈133 °C is an artifact. The first transition is endothermal, and the related peak temperature increases from 133 °C for R = butyl to 150−170 °C for the longer alkyl chains. The second transition is exothermal, and the related temperature increases from 139 °C for R = butyl to ≈160−170 °C for the longer alkyl chains. The third transition is again endothermal, and the peak temperature increases from 154 °C for R = butyl to 170−180 °C for the longer alkyl chains. Changes of the transition temperatures observed by DSC are also visible at the corresponding temperature values and heating rates in the optical microscope: at the temperature of the first endothermal transition, the solids transform into an isotropic (i.e., nonbirefringent) liquid. At the temperature of the exothermal transition, birefringent crystals appear that turn, at the temperature of the second endothermal transition, into an isotropic liquid. We attribute the first endothermal peak to melting and concomitant decomposition of $[Pt(NH_2R)_4][PtCl_4]$, and the exotherm to the crystallization of a decomposition product, which subsequently decomposes at the temperature characterized by the second endothermal peak. For alkyl chain lengths up to 9 carbon atoms, no phase transitions were observed in DSC diagrams of $[Pt(NH_2R)_4][PtCl_4]$ before melting/decomposition. The complex with R = decyl, however, displays endotherms at around 43, 60 (very weak), and 99 °C, that with R = dodecyl (Figure 5) has endotherms at 64, 75 (very weak), 96, and 113 °C (very weak), and that with R = tetradecyl has endotherms at 96 and 105 °C. All transitions except the very weak at 60 °C for the compound with R = decyl were reversible. However, the peak at 34 °C for R = decyl and that at 64 °C for R = dodecyl can shift by ≈5 °C in a second heating run. For comparison, linear phthalocyaninatopolysiloxanes substituted with alkoxy side chains containing 6 or 8 carbon atoms do not show any phase transition in DSC up to their decomposition temperature (≈300 °C).[77] The polymer with a side chain length of 12 carbon atoms, however, also exhibits the peak assigned to the melting at 96 °C and endothermal phase transitions below 96 °C.[77] These additional transitions were attributed to unspecified transitions from one solid state to another or melting of locally crystallized side chains.[77] Solid−solid transitions were also proposed for other rigid polymers with long alkyl side chains.[78]

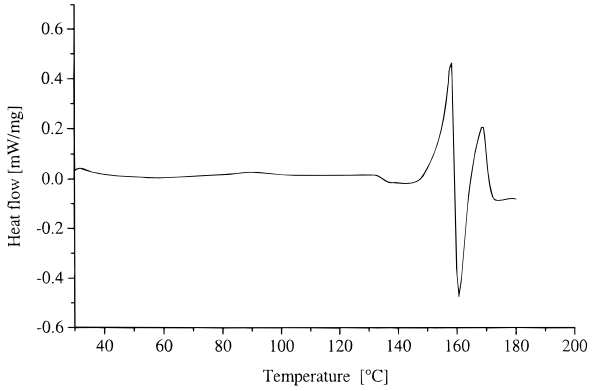

Figure 4. DSC thermogram of $[Pt(NH_2R)_4][PtCl_4]$, with R = octyl.

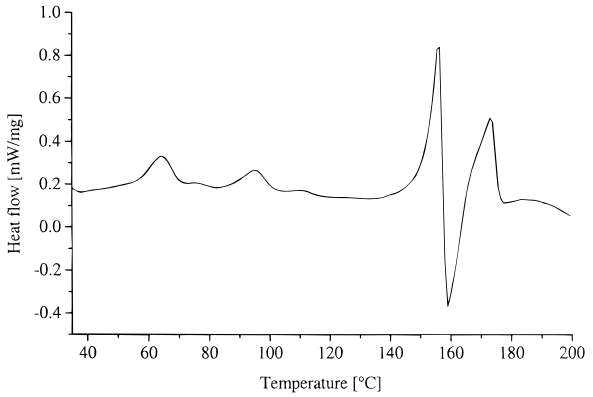

Figure 5. DSC thermogram of $[Pt(NH_2R)_4][PtCl_4]$, with R = dodecyl.

That the $[Pt(NH_2R)_4][PtCl_4]$ complexes do not melt prior to decomposition is particularly evident from DSC measurements performed at different heating rates (0.2−20 °C/min). The ratio of the integrated intensity of the first endothermal and the exothermal transition decreases with decreasing heating rate. In fact, the first

(77) Sauer, T. *Macromolecules* **1993**, *26*, 2057.
(78) Rodriguez-Parada, J. M.; Duran, R.; Wegner, G. *Macromolecules* **1989**, *22*, 2507.

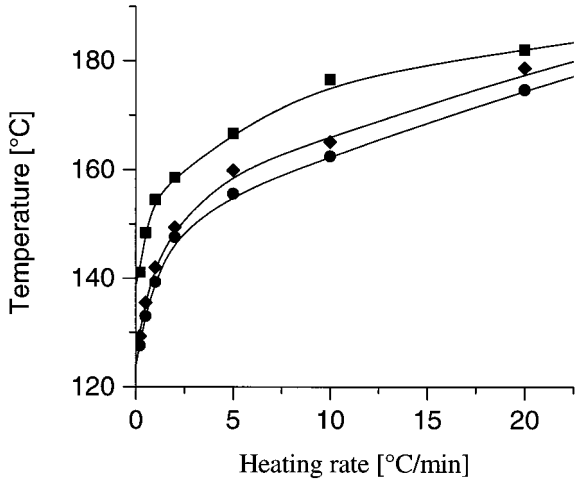

Figure 6. DSC thermogram of the first endothermal (circles), the exothermal (diamonds), and the second endothermal transition temperatures (squares) of $[Pt(NH_2R)_4][PtCl_4]$, with R = octyl, at different heating rates.

endothermal transition is hardly visible at a heating rate of 0.2 °C/min. The empirical extrapolation of the first endothermal and the exothermal transition toward a heating rate of 0 °C/min yielded identical temperatures within the precision of the method (124 and 125 °C, respectively, cf. Figure 6). The second endothermal transition becomes markedly broader with decreasing heating rate, and the determination of the related peak maximum is difficult at a heating rate of 0.2 °C/min. Qualitatively similar to the behavior of the first endothermal and the exothermal transition, the temperature of the second endothermal transition decreases with decreasing heating rate (Figure 6); however, the empirically extrapolated temperature at a heating rate of 0 °C/min of the second endothermal transition (136 °C) differs from those of the other two transitions. Hence, the phase transitions observed under typical heating rates such as 10 °C/min are strongly influenced by the kinetics of the involved processes.

Infrared Spectroscopy. The IR frequencies of the compounds of the formula $[Pt(NH_2R)_4][PtCl_4]$ are summarized in Table 4, for comparison, together with those of $[Pt(NH_2R)_4]Cl_2$ and *trans*-$[PtCl_2(NH_2R)_2]$. The IR spectra display the signals of ν(N−H) between 3210 and 3130 cm^{-1}, ν(C−H) between 2960 and 2850 cm^{-1}, $\delta(NH_2)$ between 1600 and 1570 cm^{-1}, $\delta(CH_2)$ and $\delta(CH_3)$ between 1470 and 1370 cm^{-1}, $\gamma(CH_2)$ between 740 and 720 cm^{-1}, and ν(Pt−Cl) around 320 cm^{-1}. The peak attributed to ν(Pt−N) is weak and appears at 600−605 cm^{-1}. Therefore, the substitution of a hydrogen atom in NH_3 by an alkyl group with at least 4 carbon atoms induces a shift of ν(Pt−N) by ≈100 cm^{-1} to higher frequencies (cf. Tables 2 and 4). ν(Pt−N) shifts to lower frequencies by 5 cm^{-1} in the complex with ^{15}N-labeled 1-aminododecane [$\gamma(CH_2)$, ν(C−H), $\delta(CH_2)$, $\delta(CH_3)$, $\gamma(CH_2)$, and ν(Pt−Cl) shift by 0.0−0.2 cm^{-1}, demonstrating that the shift of ν(Pt−N) is significant]. In addition, shifts to lower frequencies of 5−7 cm^{-1} are observed for the ν(N−H), and 2 cm^{-1} for $\delta(NH_2)$ in the spectra of the ^{15}N-labeled complex. The IR spectra do not particularly depend on the alkyl chain length; exceptions are $\delta(NH_2)$ in the 1-aminotetradecane complex, which is shifted by ≈10 cm^{-1} to lower frequencies, and $\gamma(CH_2)$ of the 1-aminobutane complex, which appears ≈10 cm^{-1} above the frequencies of the other homologous compounds. The wide agreement of the IR spectra indicates that the complexes of the alkyl-substituted compounds exhibit similar chemical structures.

Table 4. IR Frequencies (in cm^{-1}) of $[Pt(NH_2R)_4][PtCl_4]$ and Related Compounds for Comparison, R = $(CH_2)_nCH_3$

type of compound	*n*	ν-(N−H)	ν-(C−H)	δ-(NH_2)	$\delta(CH_2)$ $\delta(CH_3)$	γ-(CH_2)	ν-(Pt−N)	ν-(Pt−Cl)
$[Pt(NH_2R)_4]$-$[PtCl_4]$	3	3209 3131	2960 2922 2874	1591	1466 1377	733	600	319
	6	3211 3135	2958 2926 2855	1587	1466 1379	725	601	319
	7	3210 3133	2957 2924 2853	1586	1467 1378	724	605	319
	8	3210 3132	2957 2923 2853	1588	1466 1378	723	605	319
	9	3210 3133	2957 2922 2853	1587	1467 1378	722	600	321
	11	3211 3130	2958 2920 2851	1592	1468 1378	722	600	321
	13	3210 3128	2957 2920 2851	1577	1468 1378	721	605	321
$[Pt(NH_2R)_4]$-Cl_2	7	3135 3075	2958 2923 2854	1616 1594	1470 1382	725	—[a]	
trans-$[PtCl_2$-$(NH_2R)_2]$	7	3263 3230	2956 2924 2854	1588	1472 1376	718	—[a]	331
	9	3264 3230	2955 2920 2852	1588	1473 1376	717	—[a]	331

[a] Vibration not present or identified.

ν(Pt−Cl) of $[Pt(NH_2R)_4][PtCl_4]$ is close to the related frequency of Magnus' pink salt and $K_2[PtCl_4]$ and differs by ≈10 cm^{-1} from that of Magnus' green salt. This difference might indicate that the Pt−Pt distances in the alkyl substituted compounds are spaced too large for a notable Pt−Pt interaction, which probably influences ν(Pt−Cl) in Magnus' green salt. The N−H frequencies differ in the spectra of $[Pt(NH_2R)_4][PtCl_4]$ and $[Pt(NH_2R)_4]Cl_2$, which may be due to inter- or intramolecular interactions, such as weak hydrogen bonds (e.g., with chloride ligands).[76]

XPS, NEXAFS, and SAXS. The $[Pt(NH_2R)_4][PtCl_4]$ complex with R = octyl was also subjected to analysis by XPS and NEXAFS; the results are discussed next in the context of the mixed-metal complexes. We were unable to obtain single crystals suited for X-ray analysis. To favor the crystallization process, hot solutions of the complexes in toluene (10 mg/mL) were allowed to cool to room temperature and slowly dried via the gel state (vide infra) under ambient conditions. The resulting films were subjected to SAXS. The patterns of the compounds with R = decyl and dodecyl agree with those observed for a two-dimensional hexagonal lattice, calculated according to the formula[77]

$$d(hk0) = \frac{\sqrt{3D}}{2\sqrt{(h^2 + hk + k^2)}}$$

where d is the experimentally determined value of the Bragg spacing, h and k are the Miller indices in two

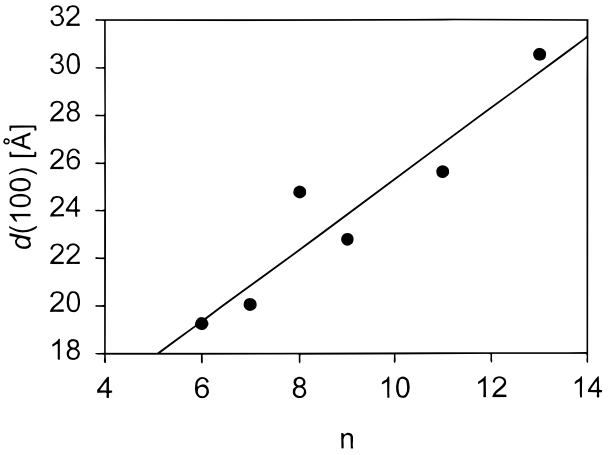

Figure 7. The $d(100)$ spacings of $[Pt(NH_2R)_4][PtCl_4]$ complexes as a function of n, the number of CH_2 groups in R.

dimensions, and D is the diameter of the hypothetical cylinder that forms the hexagonal structure. For R = decyl and dodecyl, D values of 26.2 and 29.9 Å, respectively, were calculated from the (110) reflections [$D = 2d(110)$]. The (100), (200), (300), (400), (500), (110), (210), (220)/(310), (320), and, occasionally, (600) and (330) reflections were observed [the (220) and the (310) reflections overlap at the resolution of the equipment used]. Because the X-rays are scattered by far most intensively by the Pt atoms, the two-dimensional hexagonal lattice is formed by arrays of Pt atoms. The arrays of Pt atoms are surrounded by chlorine atoms and 1-aminoalkane chains and, consequently, D is larger for R = 1-aminododecane than for 1-aminodecane.

The SAXS patterns of films of the complexes with R = heptyl, octyl, nonyl, and tetradecyl agree with a structure consisting of Pt atoms oriented in a sheet structure, where the (100), (200), (300), (400), often the (500), and occasionally the (600) reflections were observed. The (100) spacings of the $[Pt(NH_2R)_4][PtCl_4]$ complexes tend to increase with increasing chain length (Figure 7). The slope of the regression line is 1.5 Å/methylene group. The y intercept of 10 Å is close to the value of the residual $H_3C-N-Pt-N-CH_3$ unit (≈9 Å including van der Waals radii of the outer atoms), considering standard bond lengths and bond angles.

Transmission Electron Microscopy. The compound with R = heptyl was also studied with electron diffraction and TEM at high magnifications. As in SAXS, the features observed are mainly due to the Pt atoms that contribute most to the scattering of electrons. Under ordinary conditions, the metal complexes decompose within seconds under the action of electron beams typically used for TEM, as visualized by electron diffraction where an original pattern almost immediately changed into the pattern of elemental platinum. This decomposition was overcome by cooling the samples to temperatures below −175 °C during the analysis and by use of an extremely low electron flux (0.5 $e^-/Å^2$). The TEM pictures disclosed a number of regions, typically 200−1000 Å × 200−1000 Å, containing dark, parallel, elongated lines separated by 18.8 Å (Figure 8), corresponding to the (100) spacing in SAXS and the main reflex observed in electron diffraction patterns (other lines were hardly visible due to the low electron flux). Because a single array of Pt atoms is not sufficient to generate a visible contrast in an image, the dark lines must be due to parallel layers containing Pt atoms, the corresponding planes being accidentally oriented parallel to the direction of the incident electrons, analogous to the effect that provokes powder diffraction patterns.

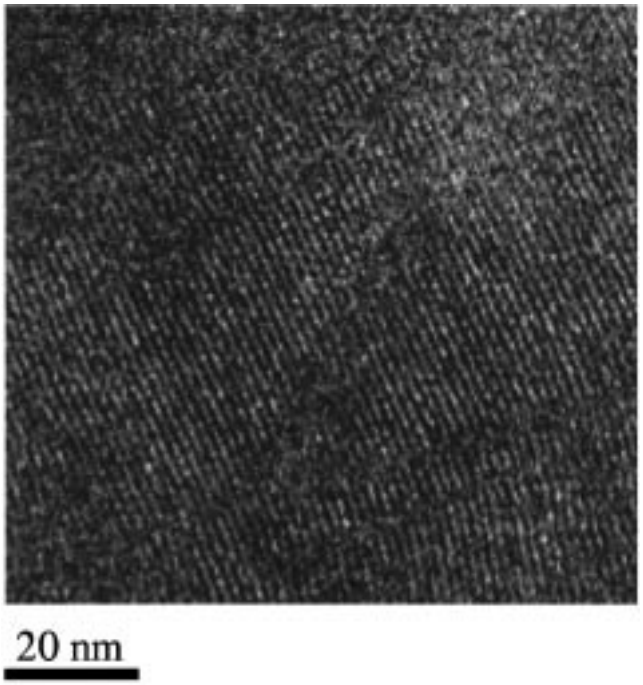

Figure 8. TEM micrograph of $[Pt(NH_2R)_4][PtCl_4]$, with R = heptyl.

Electrical Conductivity. We also attempted measurement of the electrical conductivity of the compounds with R = heptyl and octyl. Pellets of a diameter of 1.3 cm of the pure substances were pressed under a load of 10 t. The electrical conductivity was below 10^{-10} S/cm, that is, too low to be determined with our equipment.

Solubility. All $[Pt(NH_2R)_4][PtCl_4]$ complexes were insoluble or poorly soluble at room temperature in water and organic solvents such as ethanol, acetone, tetrahydrofuran, dichloromethane, chloroform, toluene, xylene, or hexane. They dissolve at room temperature under decomposition in dimethyl sulfoxide or *N*,*N*-dimethylformamide. The decomposition is accompanied by a color change, and the originally pink Pt compounds cannot be recovered from such solutions. For comparison, $[Pt(NH_2R)_4]Cl_2$ with R = octyl readily dissolves in ethanol, tetrahydrofuran, dichloromethane, chloroform, toluene, and xylene. The solubilities of the compounds of the type $[Pt(NH_2R)_4][PtCl_4]$ at the boiling temperature of the respective solvents are listed in Table 5. No solubility was found in the solvents tested for R = butyl, but the compound with R = heptyl is soluble in boiling chloroform and the compounds with even longer alkyl chains are soluble in a variety of solvents (typically, they are already soluble below the boiling temperature).

Nuclear Magnetic Resonance (NMR) Spectroscopy. The NMR spectra of the dissolved complex with R = octyl revealed little information. The peaks in the ^1H NMR spectra were broad (note that the dissolved complexes show a dynamic behavior and tend to form gels; vide infra), and couplings were not resolved. The ^{195}Pt NMR spectra of sufficient quality were not obtained in a temperature range between −60 and +90

Table 5. Solubilities ("+", soluble; "−", insoluble) at the Boiling Temperatures of the Respective Solvents of Compounds of the Type $[M^1(NH_2R)_4][M^2Cl_4]$, with R = $(CH_2)_nCH_3$

solvent	$M^1 = Pt$ $M^2 = Pt$ $n = 3$	$M^1 = Pt$ $M^2 = Pt$ $n = 6$	$M^1 = Pt$ $M^2 = Pt$ $n > 6$	$M^1 = Pd$ $M^2 = Pt$ $n = 7$	$M^1 = Pt$ $M^2 = Pd$ $n = 7$
water	−	−	−	−	−
ethanol	−	−	−	−	−
acetone	−	−	−	−	−
tetrahydrofuran	−	−	+	+	−
chloroform	−	+	+	+	−
dichloromethane	−	−	−	−	−
toluene	−	−	+	−	−
xylene	−	−	+	−	−
hexane	−	−	−	−	−

°C. Only the signals in ^{13}C NMR spectra were of satisfactory quality. The differences in the signal positions of $[Pt(NH_2R)_4][PtCl_4]$ (at room temperature in chloroform) agree typically within 0.07 ppm with those of $[Pt(NH_2R)_4]Cl_2$, except for the signals at 31.08 and 47.93 ppm, which were shifted by 0.24 ppm to lower or 0.31 ppm to higher field, respectively, in $[Pt(NH_2R)_4][PtCl_4]$. These two signals are probably associated with the carbon atoms closest to the nitrogen atom.

UV−vis Spectroscopy. The UV−vis spectrum was measured in tetrahydrofuran for the $[Pt(NH_2R)_4][PtCl_4]$ complex with R = octyl in the range 200−800 nm, and was found to be dominated by an absorption maximum (λ_{max}) at 255 nm (extinction coefficient = 23 600 $M^{-1}cm^{-1}$). On its flank, a small but clearly visible peak at 232 nm is superimposed. For comparison, $[Pt(NH_2R)_4]Cl_2$, with R = octyl, exhibits a peak at 237 nm (in $CHCl_3$) and $K_2[PtCl_4]$ exhibits one at 318 nm (in water). The value of 255 nm of $[Pt(NH_2R)_4][PtCl_4]$, with R = octyl, is close to that of the pink modification with R = ethyl (λ_{max} = 251 nm in the solid state) but distinct from that in Magnus' green salt (λ_{max} = 290 nm in the solid state) and the green modification of $[Pt(NH_2Me)_4][PtCl_4]$ (λ_{max} = 290 nm in the solid state).[37] It seems that a band at 290 nm is characteristic for the green and that at 250−255 nm is characteristic for the pink modifications. This result implies that these bands are related to intermetallic interactions of adjacent ion pairs and, therefore, to the Pt−Pt distance. Hence, we assume that the band at 255 nm indicates the presence of arrays with Pt−Pt distances in the region of that of the complex with R = ethyl (3.6 Å). The origins of the observed bands are of complex nature and have been discussed extensively in the literature.[16,17,25,36,37,61]

Gel Formation. Upon cooling to room temperature, above a certain concentration (≈0.1−0.5% w/w), the dissolved $[Pt(NH_2R)_4][PtCl_4]$ complexes formed pink gels. These gels are stable for months, although the pink color becomes somewhat darker during this period. The gelation process is thermally reversible and, hence, appears to be associated with an ordering or crystallization process. Furthermore, when observed in the optical microscope, the gels revealed birefringent, highly ordered, fibrillar structures (Figure 9). Transmission electron micrographs of dried gels show fibrillar structures resembling a collapsed network (Figure 10). The widths of the fibrillar structures are typically between 20 nm and 3 μm. The gels lose their birefringeance above a certain temperature T_d that depends on the concentration. The T_d is also roughly the temperature at which the gels transform into fluids, and hence is attributed to simple dissolution. The T_d is displayed in Figure 11 for five compounds in *o*-xylene. In the

Figure 9. Gel of $[Pt(NH_2R)_4][PtCl_4]$, with R = heptyl, in $CHCl_3$ imaged between crossed polarizers with an optical microscope.

Figure 10. A TEM micrograph of a collapsed gel of $[Pt(NH_2R)_4][PtCl_4]$, with R = heptyl.

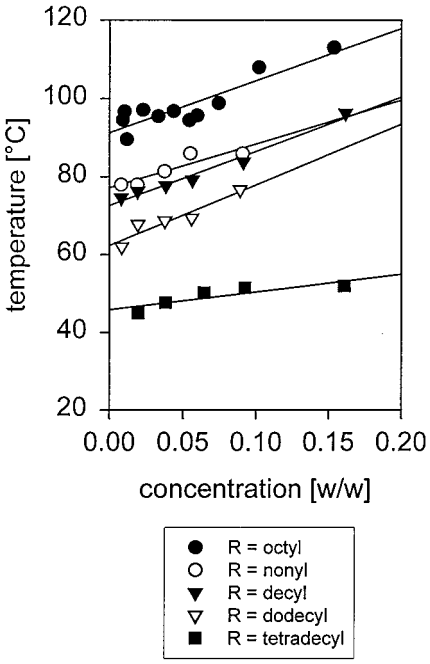

Figure 11. Temperature at which birefringeance of gels of $[Pt(NH_2R)_4][PtCl_4]$ complexes in *o*-xylene disappears, as a function of concentration.

explored range, T_d increases linearly with concentration and decreases at a given temperature with increasing chain length. For comparison, a decrease in melting and dissolution temperature with increasing length of alkyl side chains has been observed for polymers with linear (semi-)rigid backbone and flexible side chains.[77,79−82]

The IR spectra of the dried gels do not differ from those of the pristine compounds. The transition peaks observed in DSC shift by a minor difference of 2−5 °C to higher temperatures in the dried gels, which might be due to an improved order of the molecules or to larger dimensions in the dried gels. Importantly, the dried gels can again be dissolved at elevated temperatures, and the resulting solutions again form gels upon cooling to room temperature.

Gels of $[Pt(NH_2R)_4][PtCl_4]$, with R = octyl, obtained at a concentration of 3% w/w in toluene were stretched manually on glass slides to approximately twice their original length. The resulting gels were dried under ambient conditions and examined under crossed polarizers. These samples are fully extinct if the drawing axis is parallel to the polarization axis of one of the polarizers, but are highly birefringent and bright yellow when the drawing axis is oriented 45° to the polarization axes of the polarizers (Figure 12). This result demonstrates that the Pt arrays in the stretched samples are preferentially uniaxially oriented in the drawing direction. Further, fibers were manufactured from gels by electrostatic spinning.[69,83−87] Fibers, typically of 20 μm diameter, appeared in the polarization microscope similar to the films already mentioned (Figure 13), that is, they are also composed of Pt arrays uniaxially oriented in the fiber direction.

Figure 12. Film of $[Pt(NH_2R)_4][PtCl_4]$, with R = octyl, prepared by mechanical drawing in the gel state followed by solvent evaporation, imaged under crossed polarizers with an optical microscope. The drawing axis is oriented 45° to the polarization axes of the polarizers.

Mixed-Metal Compounds. $[Pt(NH_2R)_4][PdCl_4]$ was synthesized from $K_2[PdCl_4]$ and $[Pt(NH_2R)_4]Cl_2$, and $[Pd(NH_2R)_4][PtCl_4]$ by treating first $K_2[PdCl_4]$ with 1-aminooctane followed by addition of a stoichiometric amount of $K_2[PtCl_4]$. Pink solids with the expected chemical compositions were obtained. Attempts to prepare $[Pd(NH_2R)_4][PdCl_4]$ from $K_2[PdCl_4]$ and $[Pd(NH_2R)_4]Cl_2$ were not successful. The resulting yellow precipitate is suggested to consist mainly of *cis*- or *trans*-$[Pd(NH_2R)_2Cl_2]$.

In TGA (heating rate 10 °C/min), the mass loss of $[Pt(NH_2R)_4][PdCl_4]$ commences at ≈205 °C and that of $[Pd(NH_2R)_4][PtCl_4]$ begins at ≈190 °C. The maximum rate of mass loss rises at ≈230 °C for both compounds, and above ≈320 °C a constant mass of 37−38% w/w of the original mass is left, exceeding the original mass of the metals comprised (31.4% w/w), as in the case of the $[Pt(NH_2R)_4][PtCl_4]$ compounds. In the DSC diagrams (heating rate 10 °C/min), $[Pt(NH_2R)_4][PdCl_4]$ shows an irreversible, endothermal peak at 172 °C and [Pd-

(79) Moulton, J.; Smith, P. *Polymer* **1992**, *33*, 2340.
(80) Steiger, D.; Smith, P.; Weder, C. *Macromol. Rapid Commun.* **1997**, *18*, 643.
(81) Yoshino, K.; Nakajima, S.; Fujii, M.; Sugimoto, R.-I. *Polym. Commun.* **1987**, *28*, 309.
(82) Wenzel, M.; Ballauff, M.; Wegner, G. *Makromol. Chem.* **1987**, *188*, 2865.
(83) Taylor, G. *Proc. R. Soc. London, Ser. A* **1964**, *280*, 383.
(84) Taylor, G. *Proc. R. Soc. London, Ser. A* **1969**, *313*, 453.
(85) Larrondo, L.; St. John Manley, R. *J. Polym. Sci., Polym. Phys. Ed.* **1981**, *19*, 909.
(86) Larrondo, L.; St. John Manley, R. *J. Polym. Sci., Polym. Phys. Ed.* **1981**, *19*, 921.
(87) Larrondo, L.; St. John Manley, R. *J. Polym. Sci., Polym. Phys. Ed.* **1981**, *19*, 934.

Figure 13. Fiber of $[Pt(NH_2R)_4][PtCl_4]$, with R = octyl, prepared by electrostatic spinning, imaged under crossed polarizers with an optical microscope. The fiber axis is oriented 45° to the polarization axes of the polarizers.

$(NH_2R)_4][PtCl_4]$ shows one at 193 °C. Both transitions are due to decomposition of the compounds.

$[Pt(NH_2R)_4][PdCl_4]$ is insoluble in water and various organic solvents, even at their boiling temperature, whereas $[Pd(NH_2R)_4][PtCl_4]$ is soluble in boiling chloroform and tetrahydrofuran but otherwise insoluble in the solvents tested (see Table 5). The dissolved $[Pd(NH_2R)_4][PtCl_4]$ decomposes relatively quickly, accompanied by a color change from pink to yellow, and the formation of gels as in the corresponding $[Pt(NH_2R)_4][PtCl_4]$ complex was not observed. For comparison, $[Pt(NH_2R)_4]Cl_2$ is soluble at room temperature in a number of organic compounds, as already mentioned, and also $[Pd(NH_2R)_4]Cl_2$ dissolves at room temperature in dichloromethane, chloroform, and tetrahydrofuran. In hot solutions, $[Pd(NH_2R)_4]Cl_2$ is less stable than $[Pt(NH_2R)_4]Cl_2$.

The IR spectra of the mixed metal complexes $[Pt(NH_2R)_4][PdCl_4]$ and $[Pd(NH_2R)_4][PtCl_4]$ clearly differ from each other, in particular the frequencies of ν(N−H), $\delta(NH_2)$, and ν(M-Cl) (cf. Table 6). In addition, the spectrum of $[Pt(NH_2R)_4][PdCl_4]$ contains two, and that of $[Pd(NH_2R)_4][PtCl_4]$ one signal for $\delta(NH_2)$. The ν(Pt−Cl) of $[Pd(NH_2R)_4][PtCl_4]$ corresponds to the analogous

Table 6. IR Frequencies (in cm^{-1}) of $[M^1(NH_2R)_4][M^2Cl_4]$ and Related Compounds, with R = $(CH_2)_7CH_3$

type of compound	ν-(N−H)	ν-(C−H)	δ-(NH_2)	$\delta(CH_2)$ $\delta(CH_3)$	γ-(CH_2)	ν-(M−N)	ν-(M-Cl)
$[Pt(NH_2R)_4]$-$[PdCl_4]$	3134 3076	2957 2923 2854	1615 1595	1469 1378	725	—[a]	326
$[Pd(NH_2R)_4]$-$[PtCl_4]$	3227 3140	2957 2924 2854	1584	1467 1379	723	—[a]	318
$[Pd(NH_2R)_4]$-Cl_2	3282 3221 3143	2951 2920 2849	1587	1469 1376	721	—[a]	336
$K_2[PdCl_4]$[b]							336

[a] Not present or identified. [b] Reference 75.

frequency in the IR spectrum of $[Pt(NH_2R)_4][PtCl_4]$ (R = octyl). In contrast to the related $[Pt(NH_2R)_4][PtCl_4]$ complex, ν(N−H) and $\delta(NH_2)$ in the IR spectrum of $[Pt(NH_2R)_4][PdCl_4]$ coincide with the corresponding frequencies in $[Pt(NH_2R)_4]Cl_2$. Compared with ν(Pd−Cl) of $K_2[PdCl_4]$, the related frequency of $[Pt(NH_2R)_4]$-$[PdCl_4]$ is shifted by 10 cm^{-1} to lower wavelengths. The ν(N−H) and $\delta(NH_2)$ in the IR spectrum of $[Pd(NH_2R)_4]$-$[PtCl_4]$ strongly differ from the corresponding frequencies of $[Pt(NH_2R)_4]Cl_2$, but agree with those of $[Pd(NH_2R)_4]Cl_2$, the only exception being the peak at 3282 cm^{-1}, which is missing in the spectrum of $[Pd(NH_2R)_4]$-$[PtCl_4]$. However, the neighboring signal at 3227 cm^{-1} in $[Pd(NH_2R)_4][PtCl_4]$ is broad (in contrast to that at 3140 cm^{-1}). The comparisons just presented indicate that $[Pt(NH_2R)_4]^{2+}$ or $[Pd(NH_2R)_4]^{2+}$, respectively, are indeed present in $[Pt(NH_2R)_4][PdCl_4]$ and $[Pd(NH_2R)_4]$-$[PtCl_4]$, respectively.

The mixed-metal complexes, $[Pt(NH_2R)_4][PtCl_4]$, $[M(NH_2R)_4]Cl_2$, Magnus' pink salt, and $K_2[MCl_4]$, with M = Pt or Pd and R = octyl, were subjected to XPS. The reproducibility of the measured binding energies was 0.1 eV, however, it has to be noted that the peak widths were in the usual range of X-ray photoelectron spectra, i.e., by far >0.1 eV. Therefore, peaks separated by 1−2 eV are often not resolved or appear as shoulders. The obtained binding energies (Table 7) depend only moderately on the chemical nature of the compounds. The positions of the Pt($4f_{5/2}$) and Pt($4f_{7/2}$) signals are identical within the experimental precision in the spectra of $K_2[PtCl_4]$ and $[Pt(NH_2R)_4]Cl_2$. Therefore, it is not surprising that the binding energies of the different Pt atoms in $[Pt(NH_2R)_4][PtCl_4]$ and Magnus' pink salt are not resolved. Significant differences in binding energies are observed only in a few cases. The positions of the N(1s), Pt($4f_{5/2}$), and Pt($4f_{7/2}$) signals of the mixed-metal complexes differ slightly. The Cl($2p_{1/2}$) and Cl($2p_{3/2}$) binding energies in the mixed-metal complexes and in $[Pt(NH_2R)_4][PtCl_4]$ are shifted by 0.4−0.5 eV to lower energies compared with the values of the corresponding $K_2[MCl_4]$ compounds. This shift is more pronounced in the case of Magnus' pink salt (0.7 eV). The N(1s) binding energies of the complexes with the $[Pd(NH_2R)_4]^{2+}$ moieties are shifted by a small difference of 0.3 eV to lower energies, compared with the analogous complexes containing Pt. The Pt($4f_{5/2}$) and Pt($4f_{7/2}$) binding energies differ slightly in the mixed metal complexes, whereas the Pd($3d_{3/2}$) and Pd($3d_{5/2}$) binding energies do not differ significantly.

The three complexes of the type $[M^1(NH_2R)_4][M^2Cl_4]$ (with R = octyl), the potassium tetrachlorometalates(II),

Table 7. Binding Energies [eV] (from XPS) in Various Platinum and Palladium Complexes (R = octyl)

compound	N(1s)	Cl($2p_{1/2}$)	Cl($2p_{3/2}$)	Pt($4f_{5/2}$)	Pt($4f_{7/2}$)	Pd($3d_{3/2}$)	Pd($3d_{5/2}$)
Magnus' pink salt	399.8	199.4	197.8	75.4	72.1		
$[Pt(NH_2R)_4][PtCl_4]$	400.1	199.7	198.1	75.6	72.3		
$[Pt(NH_2R)_4][PdCl_4]$	400.1	199.4	197.8	75.8	72.5	343.1	337.8
$[Pd(NH_2R)_4][PtCl_4]$	399.8	199.6	198.0	75.4	72.1	343.3	338.0
$[Pt(NH_2R)_4]Cl_2$	400.1	199.2	197.6	75.7	72.4		
$[Pd(NH_2R)_4]Cl_2$	399.8	199.4	197.8			343.4	338.1
$K_2[PtCl_4]$		200.1	198.5	75.7	72.5		
$K_2[PdCl_4]$		199.9	198.3			343.5	338.3

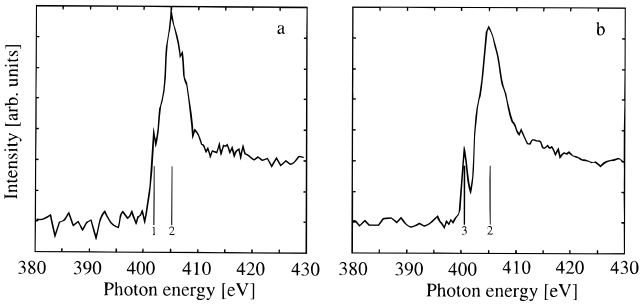

Figure 14. The NEXAFS spectra of N(1s) edges of (a) $[Pt(NH_2R)_4][PdCl_4]$, with R = octyl, and (b) $[Pd(NH_2R)_4][PtCl_4]$, with R = octyl, at normal incidence. Resonances are indicated by lines (see text).

and the tetrakis(1-aminooctane)metalate(II) dichlorides were also investigated by NEXAFS. This synchrotron-based technique probes transitions of core electrons into unoccupied molecular orbitals and hence yields information on the electronic structure of the samples. The resulting intensities are governed by dipole transition rules.

The NEXAFS spectra were recorded at the C(1s), N(1s), and Cl(2p) edges. As an example, Figure 14a shows the N(1s) edge of $[Pt(NH_2R)_4][PdCl_4]$, with R = octyl, at normal incidence of the X-rays. The spectrum shows a pronounced feature at 405.2 eV (designated 2). Moreover, a sharp shoulder can be distinguished at 402.1 eV (designated 1). On the chlorine edge (not shown), a strong resonance is situated at 202.4 eV. A very weak shoulder might be discernible at 201.3 eV. The C(1s) edge (not shown) resembles that of hydrocarbon chains of other substances, such as alkanethiols. The usual CH* and CC σ* resonances are found at 287.6, 293.1, and 301 eV.

For comparison, the N(1s) spectrum of $[Pd(NH_2R)_4][PtCl_4]$, with R = octyl, is displayed in Figure 14b. It clearly differs from the spectrum of $[Pt(NH_2R)_4][PdCl_4]$. In particular, a pronounced resonance appears at 400.7 eV (designated 3), whereas the strong transition at 405.2 eV (2) is still present, but no peak corrsponding to 1 is observed. On the chlorine edge (not shown), the situation is similar. A new peak at 200.2 eV can be resolved in addition to the transition at 202.4 eV. As expected, the transitions on the carbon edge are identical to those already described.

The examples of spectra given here represent two classes of spectra: The spectrum of $[Pd(NH_2R)_4]Cl_2$ resembles that of $[Pd(NH_2R)_4][PtCl_4]$, with distinct resonances at the nitrogen and chlorine edges. These resonances are not found in the corresponding spectra of $[Pt(NH_2R)_4]Cl_2$, $[Pt(NH_2R)_4][PtCl_4]$, and both Magnus' salts, which are very similar to the spectra of $[Pt(NH_2R)_4][PdCl_4]$. The N and Cl spectra are therefore characteristic for the metal atom to which the nitrogen atoms are coordinated, thus allowing determination of whether the nitrogen atoms coordinate to Pt or Pd. In particular, N(1s) and Cl(2p) peaks at 400.7 and 200.2 eV, respectively, are resolved when $[Pd(NH_2R)_4]^{2+}$ units are present. Because these peaks arise in the spectra of $[Pd(NH_2R)_4][PtCl_4]$ as well as that of $[Pd(NH_2R)_4]Cl_2$, they cannot be due to Pd−Pt interactions but rather to electrostatic interactions between chlorine atoms with negative (partial) charge and nitrogen atoms with positive (partial) charge. This result indicates that the chlorine and the nitrogen atoms in $[Pd(NH_2R)_4][PtCl_4]$ are separated by not more than a few angstroms. The corresponding N(1s) signal in the complexes with $[Pt(NH_2R)_4]^{2+}$ units [402.1 eV (1)] is shifted toward the energy of the transition at 405.2 eV (2) and obviously not resolved anymore in the related Cl(2p) spectra. The Cl(2p) transitions were observed exclusively in the spectra of the compounds containing nitrogen; for $K_2[MCl_4]$ only the K(2p) signals at 297.2 and 300.0 eV were visible.

Discussion

$[Pt(NH_3)_4][PtCl_4]$ exists in two modifications that can be distinguished visually by their color. The green modification (Magnus' green salt) has been well characterized in the literature (see Introduction). It contains linear arrays of Pt atoms separated by 3.23−3.25 Å.[16,25,26] The pink modification, designated Magnus' pink salt (although it is not clear if it ever was prepared by Magnus at all; see *Introduction*), found less attention. Its synthesis is less straightforward than that of Magnus' green salt. According to our experiments, at 0 °C the pink modification forms and at high temperatures, predominantly the green modification forms. Hence, the green salt seems to be the more stable modification. It has not been possible to date to obtain crystals of Magnus' pink salt that are suited for single-crystal XRD analysis, but powder diffraction patterns show that the closest Pt−Pt distance in Magnus' pink salt is >5 Å.[26] Therefore, the structure of the green and the pink modification must differ markedly, which is also evident from IR spectra (cf. Table 2). The ν(Pt−Cl) and ν(Pt−N) in Magnus' pink salt agree with those in $K_2[PtCl_4]$ and $[Pt(NH_3)_4]Cl_2$, respectively, indicating that Magnus' pink salt indeed consists of $[PtCl_4]^{2-}$ and $[Pt(NH_3)_4]^{2+}$ units and that these units do not interact strongly via Pt−Pt bonds (note that ν(Pt−Cl) of Magnus' green salt differs from that of $K_2[PtCl_4]$). However, differences in $\delta(NH_3)$ and $\rho(NH_3)$ in IR spectra (cf. Table 2) and in Cl($2p_{1/2}$) and Cl($2p_{1/2}$) binding energies (cf. Table 7) indicate that the state of the complex ions in Magnus' pink salt is not exactly the same as in those in $K_2[PtCl_4]$ and $[Pt(NH_3)_4]Cl_2$, respectively. It has been calculated that the interactions between the complex ions in Magnus' green salt are described more adequately by

an ion pair model than with a model in which Pt−Pt bonds play a dominant role.[35] The Pt−Pt interactions occur, but are only weak,[35] which is not surprising for a d^8 center that favors a square planar coordination sphere. Although adjacent coordination units are attracted by their opposite charges, the effective charges of Pt in the $[PtCl_4]^{2-}$ and $[Pt(NH_3)_4]^{2+}$ units are 0.44+ and 0.56+, respectively.[35] Hence, a certain activation energy might be required to overcome the electrostatic repulsion between adjacent platinum atoms, which may allow a kinetically controlled formation of a modification with larger Pt−Pt distances.

Only one modification has been characterized so far for each of the complexes of the type $[Pt(NH_2R)_4][PtCl_4]$, with R = alkyl. The complex with R = methyl is green,[36,47,60−64] and is of a structure and exhibits Pt−Pt distances such as in Magnus' green salt.[16,25,62] The compounds with R = ethyl, propyl, and butyl,[36,61−64] as well as those with R ranging from heptyl to tetradecyl prepared in this work, are pink. We conclude that, based on the extensive results presented here, reports on modifications of brown-yellow,[60] brown,[65] and greenish-grey[63] modifications are erroneous. Only the pink complex with R = ethyl could be analyzed with single-crystal X-ray analysis,[62] revealing linearly arranged Pt atoms with an intermetallic distance of 3.62 Å. It seems, therefore, that the structure in the compound with R = ethyl is more closely related to the Magnus' green than the pink salt, and that the compounds that share the pink color are not always isostructural. The green color indeed seems to be restricted to compounds with the shorter Pt−Pt distances and the resulting (still weak) Pt−Pt bonds. The UV spectra of the green complexes are dominated by a band at 290 nm, which is lacking in the alkyl-substituted pink modifications. The pink modifications with alkyl substituents seem to exhibit a characteristic absorption maximum of the most intensive band at 250−255 nm.

$[Pd(NH_3)_4][PdCl_4]$ (Vauquelin's salt), $[Pd(NH_3)_4][PtCl_4]$, and $[Pt(NH_3)_4][PdCl_4]$ exhibit the same structures and intermetallic distances as Magnus' green salt,[16,25,36,47] but all complexes containing Pd are pink. This result might be associated with reduced intermetallic interactions in the complexes with Pd (e.g., in diatomic molecules the bond dissociation energy of Pd−Pd is 100 kJ/mol and that of Pt−Pt is 357 kJ/mol[88]), due to the relative sizes of the atomic orbitals of the Pt and Pd atoms.[36] It has also been suggested that 4*f* orbitals might contribute to the Pt−Pt interactions in Magnus' green salt.[36]

The conformity of the IR spectra and the melting/decomposition behavior disclosed by DSC measurements suggest a similar structure for the complexes with R ranging from butyl to tetradecyl. The comparison of $[Pt(NH_2R)_4][PtCl_4]$ with $[Pt(NH_2R)_4]Cl_2$ by NEXAFS leads to the conclusion that $[Pt(NH_2R)_4][PtCl_4]$ is indeed composed of $[Pt(NH_2R)_4]^{2+}$ (and $[PtCl_4]^{2-}$) units. The IR spectra agree with this suggestion. The color of the complexes with 4−14 carbon atoms in the alkyl chains coincides with that of the compounds with larger Pt−Pt spacings (R = ethyl and Magnus' pink salt) but markedly differs from that of the complexes with Pt−Pt spacings around 3.25 Å (R = methyl and Magnus' green salt). We conclude from all those observations that the Pt atoms in the substances containing 4−14 carbon atoms in the alkyl chains are separated by >3.25 Å. It has been estimated that energies of *d*−*d* transitions can be highly sensitive to differences in Pt−Pt spacings in the region 3.25−3.6 Å.[16] The UV spectrum of the complex with R = octyl is not simply composed of a superposition of the λ_{max} of the model compounds $[Pt(NH_2R)_4]Cl_2$ and $K_2[PtCl_4]$, indicating that very weak Pt−Pt interactions are present also in the pink alkyl-substituted compounds. Indeed, the UV spectrum of R = ethyl shows its main absorption very close to the corresponding wavelength in the complex with R = octyl. We, therefore, arrived at the conclusion that the Pt−Pt distance in the compound with R = octyl should be similar to that with R = ethyl (i.e., around 3.6 Å). At this distance, weak Pt−Pt interactions in a complex with stacked $[Pt(NH_2R)_4]^{2+}$ and $[PtCl_4]^{2-}$ have still been predicted to exist by model calculations.[35] Due to the weak Pt−Pt interactions, the $Pt[(NH_2R)_4][PtCl_4]$ complexes might also be considered as self-assembled supramolecular structures.

Measurements of the electrical conductivity indicate that the Pt−Pt distance in the compounds with R = heptyl and octyl is above that of Magnus' green salt. Although the electrical conductivity of Magnus' green salt reported in the literature varies over several orders of magnitude ($\approx 10^{-2} - 10^{-8}$ S/cm),[21,39−44] the conductivities of the pink compounds with R = heptyl and octyl are clearly lower.

Based on SAXS studies of polycrystalline samples, the Pt atoms in the complexes with R = decyl and dodecyl form linear arrays arranged in a two-dimensional hexagonal structure (Figure 15). The distance between the Pt arrays is determined by the alkyl chains. The structure of the complexes with R = decyl and dodecyl corresponds, for example, to the lattice formed by rodlike phthalocyaninatopolysiloxanes with flexible side chains.[77] The substances with R = heptyl, octyl, nonyl, and tetradecyl contain Pt atoms arranged in parallel sheets. The spacing between adjacent sheets is determined by the length of the alkyl chains, but this dependence is not necessarily linear (vide infra). It appears that these sheets are formed again by linear arrays of Pt atoms, separated by the coordinated 1-aminoalkanes, analogous to, for example, the structure of several organic polymers with a linear, organic backbone with attached alkoxy side chains.[78,82,89] Although the driving force for the formation of Pt arrays may be regarded as a consequence of the ionic interaction in stacks of alternatively charged ion pairs, the relation between those arrays is probably determined by the interactions of the alkyl chains with each other. For example, crystallization of alkyl chains within the arrays and between the arrays is possible. The distribution between those two types of crystallization can depend on the alkyl chain length, and as a consequence sheet or hexagonal structures may be favored at particular chain lengths or crystallization conditions. The DSC diagrams disclose reversible transitions for R = decyl, dodecyl, and, to a lesser extent, tetradecyl. These transitions might be

(88) *Handbook of Chemistry and Physics, 76th ed.*; Lide, D. R., Ed.; CRC Press: Boca Raton, FL, 1995.

(89) Weder, C.; Wrighton, M. S. *Macromolecules* **1996**, *29*, 5157.

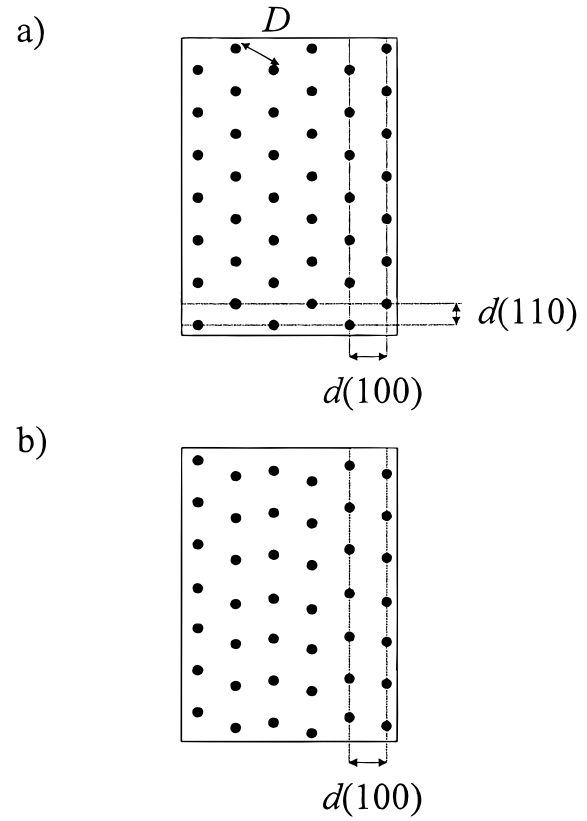

Figure 15. Schematic illustration of the cross section perpendicular to the Pt arrays in bulk $[Pt(NH_2R)_4][PtCl_4]$ (the circles represent the sectioned arrays): (a) hexagonal arrangement for R = decyl and dodecyl; (b) linear arrangement for R = heptyl, octyl, nonyl, and tetradecyl.

associated with the melting of locally crystallized side chains or to transitions in different solid-state modifications (e.g. in the case of R = decyl and dodecyl from hexagonal to sheet structures). In those structures, a strictly linear dependence of the (100) spacings on the alkyl side chain length is expected only if all the complexes crystallized in the same structure (which is obviously not the case) and if the Pt−Pt spacings were constant in all the compounds examined. Besides the ionic interactions, the crystallization of alkyl chains may also influence the Pt−Pt distance.[62]

Despite the presumably weak intermetallic interactions in the main chain, the $[Pt(NH_2R)_4][PtCl_4]$ also show characteristics of rigid rod polymers. As expected, on the basis of the knowledge on rigid rod polymers, the solubility and processability of $[Pt(NH_2R)_4][PtCl_4]$ increases for complexes with longer alkyl chains:[77,79−81,90] the complex with R = butyl is insoluble in all the solvents tested at their boiling temperatures; that with R = heptyl dissolves in hot chloroform but is otherwise insoluble; and the complexes with alkyl chains containing >7 carbon atoms dissolve in several hot solvents. However, in contrast to the general behavior of rigid rod polymers with flexible side chains, none of the $[Pt(NH_2R)_4][PtCl_4]$ compounds prepared here undergoes a transition in the liquid crystalline state.

Interestingly, the $[Pt(NH_2R)_4][PtCl_4]$ complexes form gels upon cooling. The existence of a gel phase depends on the concentration of the Pt complex and the temperature. At a given concentration, the temperature at which the gels transform into a fluid phase decreases with increasing chain length, indicating that the alkyl chains are a major factor in the formation of the gels. The gelation process is thermo-reversible, and the gels contain ordered structures in contrast to the fluid phases. The fluid phases would be birefringent if they contained individual Pt arrays above a certain aspect ratio and, therefore, molecular length.[91] For a volume fraction of 0.1 and a molecular diameter of $[Pt(NH_2R)_4][PtCl_4]$ of 20 Å, this maximum molecular length can be calculated to 1500 Å,[91] that is, far below the length of the fibrillar structures in the gels. On the other hand, the gels might not be formed by association of preformed arrays but by growth of individual fragments to fibrillar structures. In both cases, the fibrillar structures are expected to decay at elevated temperatures. The structure of the fibrilles in the $[Pt(NH_2R)_4][PtCl_4]$ gels is determined by interactions of the alkyl chains coordinated to neighboring arrays of platinum atoms and by interactions of the alkyl side chains with the solvent. The longer the alkyl side chains, the higher the entropy loss upon formation of the ordered, fibrillar structures, that is, the temperature at which the gels form decreases with increasing chain length. However, it has to be considered that electrostatic interactions may influence the intermetallic distance and, therefore, the packing of the alkyl chains attached to metal atoms. This influence might be the reason for the differences in the solubilities of $[Pt(NH_2R)_4][PtCl_4]$, $[Pd(NH_2R)_4][PtCl_4]$, and $[Pt(NH_2R)_4][PdCl_4]$. Oriented fibrillar structures in the gels can be obtained mechanically by drawing or by electrostatic spinning.

$[Pd(NH_2R)_4][PtCl_4]$ and $[Pt(NH_2R)_4][PdCl_4]$ (R = octyl) differ in their thermal stability, solubility, vibrational frequencies, and energies of electronic transitions, as revealed by NEXAFS. There is evidence from NEXAFS and IR spectroscopy that the mixed metal complexes are indeed composed of the respective complex ions and that electrostatic interactions between nitrogen and chlorine atoms are present. Although $[Pd(NH_2R)_4][PtCl_4]$ decomposes far above 100 °C, its stability is limited in solution, whereas $[Pd(NH_2R)_4][PtCl_4]$ in our limited study was insoluble at all temperatures studied.

The synthesis of $[Pd(NH_2R)_4][PdCl_4]$ by combination of aqueous solutions of $[Pd(NH_2R)_4]^{2+}$ and $[PdCl_4]^{2-}$ failed to yield the desired complex. Palladium complexes are frequently less inert than Pt complexes. For instance, dissolved $[Pd(NH_2R)_4]Cl_2$ decomposes faster at elevated temperatures than $[Pt(NH_2R)_4]Cl_2$. The decomposition of $[Pd(NH_2R)_4]^{2+}$ moieties may, therefore, be induced in solution by dissociation of 1-aminoalkane, which may substitute a chloride ion in $[PdCl_4]^{2-}$ via an associative mechanism, finally resulting in complexes containing both chloride and 1-aminoalkane in the ligand sphere. Note that a main product of the thermal decomposition of $[Pt(NH_2R)_4][PtCl_4]$ is *trans*-$[Pt(NH_2R)_2Cl_2]$. This result indicates that $[Pt(NH_2R)_4][PtCl_4]$ is not the most stable isomer but the product that forms first under our reaction conditions.

(90) Postema, A. R.; Liou, K.; Wudl, F.; Smith, P. *Macromolecules* **1990**, *23*, 1842.

(91) Flory, P. J. *Proc. R. Soc. London, Ser. A* **1956**, *234*, 73.

Conclusions

$[Pt(NH_3)_4][PtCl_4]$ exists in a pink modification (Magnus' pink salt), the formation of which is kinetically favored, and in a green modification that appears to be thermodynamically more stable. In $[Pt(NH_2R)_4][PtCl_4]$ complexes, only one modification has been isolated to date for a specified R: green for R = methyl and pink for the higher chain lengths. The compounds of the type $[Pt(NH_2R)_4][PtCl_4]$ (R = butyl, heptyl, octyl, nonyl, decyl, dodecyl, and tetradecyl), and the mixed metal complexes $[Pd(NH_2R)_4][PtCl_4]$ (R = octyl) and $[Pt(NH_2R)_4][PdCl_4]$ (R = octyl) can be prepared as pure compounds that decompose at a heating rate of 10 °C/min at 140−195 °C, depending on the complex. The complexes with the different metal atoms can be distinguished with IR spectroscopy and NEXAFS, which reveal that the complexes are indeed composed of the related complex ions.

Although the compounds of the type $[Pt(NH_2R)_4][PtCl_4]$, where R is an alkyl chain longer than methyl, are pink, their structure is most likely related to the complex with R = methyl and to Magnus' green salt rather than to Magnus' pink salt. It seems that the green color indicates weak Pt−Pt bonds that are, however, dominated by electrostatic interactions. In the alkyl-substituted pink complexes, Pt−Pt interactions are still present but even weaker than in Magnus' green salt. The Pt−Pt distances of the compounds in the pink modifications with the 1−aminoalkanes are likely to be in a range of 3.6 Å, although this distance could only be determined experimentally for R = ethyl. Hence, the related complexes may be attributed to the class of self-assembled supramolecular structures.

Interactions between alkyl chains are important not only for the type of structure formed in their solid phase but also for the properties of the compounds in solution. Complexes with short alkyl chains are insoluble but become soluble for longer chains, analogous to the behavior of rigid rod polymers with flexible side chains. Like these polymers, the Pt complexes form two-dimensional hexagonal and sheet structures, depending on the particular chemical composition of the molecules. However, these phase-properties of the Pt complexes are not equivalent to those of the rigid polymers. Rigid rod polymers of sufficient length with flexible side chains frequently form liquid crystalline phases, which were not observed for the Pt complexes. Also, $[Pt(NH_2R)_4][PtCl_4]$ complexes with longer chains might form gels with fibrillar structures via a mechanism different from gel formation of rigid rod polymers. In solution, the arrays in $[Pt(NH_2R)_4][PtCl_4]$ might be in equilibrium with fragments (e.g., ion pairs), whereas the main chain in rigid rod polymers is, of course, of constant length during the gelation process. Gelation of the $[Pt(NH_2R)_4][PtCl_4]$ enables the formation of most interesting films and fibers comprising uniaxially oriented fibrils in which the Pt−Pt images are oriented in the deformation direction.

Bulk mixed-metal $[Pd(NH_2R)_4][PtCl_4]$ (R = octyl) decomposes at a heating rate of 10 °C/min even at higher temperature than the corresponding Pt complex, but in solution the Pd complex decomposes much faster, due to the lability of the Pd compounds compared with the inertness of the respective Pt compounds. $[Pt(NH_2R)_4][PdCl_4]$ is insoluble, at least in the solvents tested. Both $[Pt(NH_2R)_4][PtCl_4]$ as well as the mixed metal complexes are metastable; most likely the *trans*-dichlorobis(1-aminoalkane)metal(II) compounds would dominate in the equilibrium. In the case of dissolved $[Pd(NH_2R)_4][PtCl_4]$ the activation energy is sufficiently low to allow the related conversion quickly. The lability of the Pd compounds even prevented the preparation of $[Pd(NH_2R)_4][PdCl_4]$ under similar conditions as used for the synthesis of the other complexes described here.

Acknowledgment. We are indebted to V. Gramlich for performing X-ray single crystal structure analysis, A. Häne and Y. Städler for experimental assistance, and H. Gross and P. Tittmann for carrying out TEM. We also thank U. W. Suter for helpful discussions and the ETH, which supported this work within the framework of the project "Templated Materials" (TEMA). NEXAFS measurements were performed at the NSLS (Brookhaven, NY), which is supported by the U. S. Department of Energy.

Appendix

Crystal Structures for Complexes of the Type $[Pt(NH_2R)_4][PtCl_4]$ R = Octyl. See Figure 16 and Tables 8−12.

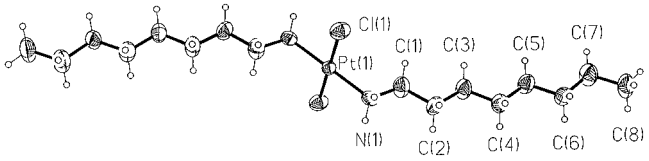

Figure 16. A view of the molecular structure of *trans*-$[Pt(NH_2R)_2Cl_2]$, with R = octyl.

Table 8. Crystal Data and Structure Refinement

empirical formula	$C_{16}H_{38}Cl_2N_2Pt$
formula weight	524.47
temperature	293(2) K
wavelength	0.71073 Å
crystal system	monoclinic
space group	P2(1)/c
unit cell dimensions	a = 14.273(6) Å α = 90°
	b = 8.244(4) Å β = 100.69(4)°
	c = 9.145(5) Å γ = 90°
volume	1057.4(9) Å^3
Z	2
density (calculated)	1.647 Mg/m^3
absorption coefficient	6.885 mm^{-1}
F(000)	520
crystal size	0.8 × 0.35 × 0.35 mm
θ range for data collection	2.87−20.04°
index ranges	$-13 \le h \le 13$, $0 \le k \le 7$, $0 \le l \le 8$
reflections collected	801
independent reflections	801 [R(int) = 0.0000]
absorption correction	integration
max. and min. transmission	0.1343 and 0.0189
refinement method	full-matrix least-squares on F^2
data/restraints/parameters	801/0/117
goodness-of-fit on F^2	1.054
final R indices [$I > 2F(I)$]	R1 = 0.0238, wR2 = 0.0611
R indices (all data)	R1 = 0.0238, wR2 = 0.0611
extinction coefficient	0.0017(8)
largest diff. peak and hole	1.111 and −0.925 eÅ^{-3}

Table 9. Bond Lengths [Å] and Angles [deg][a]

Pt(1)−N(1)#1	2.038(7)	C(4)−C(3)	1.512(10)
Pt(1)−N(1)	2.038(7)	C(7)−C(8)	1.508(11)
Pt(1)−Cl(1)	2.297(2)	C(7)−C(6)	1.513(11)
Pt(1)−Cl(1)#1	2.297(2)	C(3)−C(2)	1.502(10)
N(1)−C(1)	1.498(10)	C(6)−C(5)	1.509(10)
C(4)−C(5)	1.495(10)	C(2)−C(1)	1.505(11)
N(1)#1−Pt(1)−N(1)	180.0	C(5)−C(4)−C(3)	113.5(7)
N(1)#1−Pt(1)−Cl(1)	89.7(2)	C(8)−C(7)−C(6)	115.3(8)
N(1)−Pt(1)−Cl(1)	90.3(2)	C(2)−C(3)−C(4)	116.9(7)
N(1)#1−Pt(1)−Cl(1)#1	90.3(2)	C(5)−C(6)−C(7)	114.2(8)
N(1)−Pt(1)−Cl(1)#1	89.7(2)	C(3)−C(2)−C(1)	111.0(7)
Cl(1)−Pt(1)−Cl(1)#1	180.0	C(4)−C(5)−C(6)	116.0(8)
C(1)−N(1)−Pt(1)	111.3(5)	N(1)−C(1)−C(2)	116.7(7)

[a] Symmetry transformations used to generate equivalent atoms: #1 $-x, -y, -z$.

Table 10. Atomic Coordinates ($\times 10^4$) and Equivalent Isotropic Displacement Parameters ($A^2 \times 10^3$) [U(eq) is Defined as One Third of the Trace of the Orthogonalized U_{ij} tensor]

atom	x	y	z	U(eq)
Pt(1)	0	0	0	34(1)
Cl(1)	−310(2)	−2736(3)	−58(2)	53(1)
N(1)	−663(5)	257(7)	1777(7)	39(2)
C(4)	−4018(5)	936(12)	2899(9)	57(2)
C(7)	−6790(6)	953(14)	2335(10)	72(3)
C(3)	−3327(5)	958(13)	1830(9)	58(2)
C(6)	−5766(5)	965(13)	3150(9)	56(2)
C(2)	−2289(6)	748(13)	2489(9)	54(2)
C(5)	−5040(5)	1025(13)	2145(10)	59(3)
C(8)	−7530(6)	866(17)	3313(11)	79(3)
C(1)	−1697(6)	664(13)	1290(10)	57(2)

Table 11. Anisotropic Displacement Parameters ($A^2 \times 10^3$). [The Anisotropic Displacement Factor Exponent Takes the Form $-2\pi^2[h^2a^{*2}U_{11} + \ldots + 2\,h\,k\,a^*\,b^*\,U_{12}]$]

atom	U_{11}	U_{22}	U_{33}	U_{23}	U_{13}	U_{12}
Pt(1)	33(1)	41(1)	27(1)	0(1)	5(1)	0(1)
Cl(1)	71(1)	46(1)	45(1)	−2(1)	16(1)	−8(1)
N(1)	41(4)	40(4)	34(4)	2(4)	1(3)	−5(3)
C(4)	39(6)	82(7)	51(6)	−4(6)	11(4)	4(5)
C(7)	47(7)	105(8)	63(7)	9(8)	7(5)	13(5)
C(3)	37(6)	88(7)	48(6)	6(6)	7(4)	13(5)
C(6)	39(6)	87(7)	39(6)	0(6)	3(4)	7(5)
C(2)	53(6)	73(6)	38(6)	−1(6)	18(4)	2(5)
C(5)	45(6)	91(8)	42(6)	4(6)	8(4)	11(4)
C(8)	41(7)	130(9)	68(7)	10(9)	15(5)	3(6)
C(1)	46(6)	78(6)	50(6)	12(6)	11(4)	8(5)

Table 12. Hydrogen Coordinates ($\times 10^4$) and Isotropic Displacement Parameters ($A^2 \times 10^3$)

atom	x	y	z	U(eq)
H(1C)	−373(5)	1043(7)	2379(7)	66(28)
H(1D)	−612(5)	−676(7)	2296(7)	23(19)
H(4A)	−3879(5)	1850(12)	3553(9)	90(33)
H(4B)	−3918(5)	−37(12)	3484(9)	108(51)
H(7A)	−6878(6)	52(14)	1658(10)	107(52)
H(7B)	−6896(6)	1932(14)	1760(10)	62(26)
H(3A)	−3408(5)	1963(13)	1290(9)	76(29)
H(3B)	−3510(5)	93(13)	1133(9)	61(32)
H(6A)	−5656(5)	−7(13)	3734(9)	62(32)
H(6B)	−5669(5)	1878(13)	3813(9)	124(42)
H(2A)	−2195(6)	−237(13)	3056(9)	124(52)
H(2B)	−2079(6)	1645(13)	3135(9)	76(30)
H(5A)	−5162(5)	139(13)	1454(10)	67(33)
H(5B)	−5138(5)	2018(13)	1590(10)	77(28)
H(8B)	−8164(6)	876(17)	2731(11)	95(31)
H(8C)	−7432(6)	−122(17)	3877(11)	106(50)
H(8D)	−7451(6)	1776(17)	3980(11)	137(53)
H(1A)	−1984(6)	−130(13)	578(10)	141(64)
H(1B)	−1744(6)	1701(13)	803(10)	83(31)

R = Decyl. See Figure 17 and Tables 13−17.

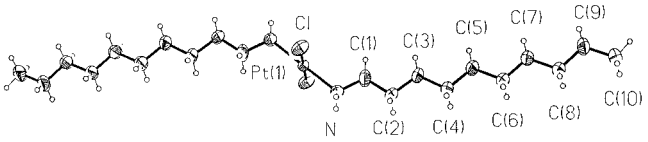

Figure 17. A view of the molecular structure of *trans*-$[Pt(NH_2R)_2Cl_2]$, with R = decyl.

Table 13. Crystal Data and Structure Refinement

empirical formula	$C_{20}H_{46}Cl_2N_2Pt$
formula weight	580.58
temperature	293(2) K
wavelength	0.71073 Å
crystal system	monoclinic
space group	P2(1)/c
unit cell dimensions	$a = 16.807(7)$ Å $\alpha = 90°$ $b = 8.218(3)$ Å $\beta = 101.26(3)°$ $c = 9.204(4)$ Å $\gamma = 90°$
volume	1246.8(9) Å^3
Z	4
density (calculated)	1.546 Mg/m^3
absorption coefficient	5.848 mm^{-1}
F(000)	584
crystal size	0.2 × 0.2 × 0.07 mm
θ range for data collection	2.47−20.02°
index ranges	$-16 \le h \le 15, 0 \le k \le 7, 0 \le l \le 8$
reflections collected	1166
independent reflections	1166 [R(int) = 0.0000]
absorption correction	integration
max. and min. transmission	0.451 and 0.179
refinement method	full-matrix least-squares on F^2
data/restraints/parameters	1166/0/116
goodness-of-fit on F^2	0.900
final R indices [$I > 2F(I)$]	R1 = 0.0318, wR2 = 0.0759
R indices (all data)	R1 = 0.0377, wR2 = 0.0783
extinction coefficient	0.0015(5)
largest diff. peak and hole	1.011 and −0.581 eÅ^{-3}

Table 14. Bond Lengths [Å] and Angles [deg][a]

Pt(1)−N	2.045(7)	C(7)−C(8)	1.514(13)
Pt(1)−N#1	2.045(7)	C(5)−C(6)	1.510(12)
Pt(1)−Cl#1	2.295(3)	C(8)−C(9)	1.503(11)
Pt(1)−Cl	2.295(3)	C(3)−C(2)	1.520(11)
C(4)−C(5)	1.519(12)	C(9)−C(10)	1.508(13)
C(4)−C(3)	1.524(12)	C(2)−C(1)	1.487(13)
C(7)−C(6)	1.506(11)	N−C(1)	1.464(11)
N−Pt(1)−N#1	180.0	C(6)−C(5)−C(4)	115.5(8)
N−Pt(1)−Cl#1	89.7(2)	C(7)−C(6)−C(5)	114.2(8)
N#1−Pt(1)−Cl#1	90.3(2)	C(9)−C(8)−C(7)	114.7(8)
N−Pt(1)−Cl	90.3(2)	C(2)−C(3)−C(4)	115.9(8)
N#1−Pt(1)−Cl	89.7(2)	C(8)−C(9)−C(10)	114.8(8)
Cl#1−Pt(1)−Cl	180.0	C(1)−C(2)−C(3)	109.9(8)
C(5)−C(4)−C(3)	113.3(8)	C(1)−N−Pt(1)	113.2(6)
C(6)−C(7)−C(8)	115.6(8)	N−C(1)−C(2)	117.2(8)

[a] Symmetry transformations used to generate equivalent atoms: #1 $-x, -y, -z$.

Table 15. Atomic Coordinates ($\times 10^4$) and Equivalent Isotropic Displacement Parameters ($A^2 \times 10^3$) [U(eq) Is Defined as One-Third of the Trace of the Orthogonalized U_{ij} Tensor]

atom	x	y	z	U(eq)
Pt(1)	0	0	0	34(1)
Cl(1)	−310(2)	−2736(3)	−58(2)	53(1)
N(1)	−663(5)	257(7)	1777(7)	39(2)
C(4)	−4018(5)	936(12)	2899(9)	57(2)
C(7)	−6790(6)	953(14)	2335(10)	72(3)
C(3)	−3327(5)	958(13)	1830(9)	58(2)
C(6)	−5766(5)	965(13)	3150(9)	56(2)
C(2)	−2289(6)	748(13)	2489(9)	54(2)
C(5)	−5040(5)	1025(13)	2145(10)	59(3)
C(8)	−7530(6)	866(17)	3313(11)	79(3)
C(1)	−1697(6)	664(13)	1290(10)	57(2)

Table 16. Anisotropic Displacement Parameters ($A^2 \times 10^3$) [The Anisotropic Displacement Factor Exponent Takes the Form $-2\pi^2[h^2 a^{*2} U_{11} + ... + 2 h k a^* b^* U_{12}]$]

atom	U_{11}	U_{22}	U_{33}	U_{23}	U_{13}	U_{12}
Pt(1)	33(1)	41(1)	27(1)	0(1)	5(1)	0(1)
Cl(1)	71(1)	46(1)	45(1)	−2(1)	16(1)	−8(1)
N(1)	41(4)	40(4)	34(4)	2(4)	1(3)	−5(3)
C(4)	39(6)	82(7)	51(6)	−4(6)	11(4)	4(5)
C(7)	47(7)	105(8)	63(7)	9(8)	7(5)	13(5)
C(3)	37(6)	88(7)	48(6)	6(6)	7(4)	13(5)
C(6)	39(6)	87(7)	39(6)	0(6)	3(4)	7(5)
C(2)	53(6)	73(6)	38(6)	−1(6)	18(4)	2(5)
C(5)	45(6)	91(8)	42(6)	4(6)	8(4)	11(4)
C(8)	41(7)	130(9)	68(7)	10(9)	15(5)	3(6)
C(1)	46(6)	78(6)	50(6)	12(6)	11(4)	8(5)

CM9806376

Table 17. Hydrogen Coordinates ($\times 10^4$) and Isotropic Displacement Parameters ($A^2 \times 10^3$)

atom	*x*	*y*	*z*	*U*(eq)
H(1C)	−373(5)	1043(7)	2379(7)	66(28)
H(1D)	−612(5)	−676(7)	2296(7)	23(19)
H(4A)	−3879(5)	1850(12)	3553(9)	90(33)
H(4B)	−3918(5)	−37(12)	3484(9)	108(51)
H(7A)	−6878(6)	52(14)	1658(10)	107(52)
H(7B)	−6896(6)	1932(14)	1760(10)	62(26)
H(3A)	−3408(5)	1963(13)	1290(9)	76(29)
H(3B)	−3510(5)	93(13)	1133(9)	61(32)
H(6A)	−5656(5)	−7(13)	3734(9)	62(32)
H(6B)	−5669(5)	1878(13)	3813(9)	124(42)
H(2A)	−2195(6)	−237(13)	3056(9)	124(52)
H(2B)	−2079(6)	1645(13)	3135(9)	76(30)
H(5A)	−5162(5)	139(13)	1454(10)	67(33)
H(5B)	−5138(5)	2018(13)	1590(10)	77(28)
H(8B)	−8164(6)	876(17)	2731(11)	95(31)
H(8C)	−7432(6)	−122(17)	3877(11)	106(50)
H(8D)	−7451(6)	1776(17)	3980(11)	137(53)
H(1A)	−1984(6)	−130(13)	578(10)	141(64)
H(1B)	−1744(6)	1701(13)	803(10)	83(31)